Entropy generation in condensation in the presence of high concentrations of noncondensable gases

Gregory P. Thiel[a], John H. Lienhard V[a,*]

[a] *Rohsenow Kendall Heat Transfer Laboratory, Department of Mechanical Engineering, Massachusetts Institute of Technology, Cambridge, MA 02139-4307, USA*

Abstract

The physical mechanisms of entropy generation in a condenser with high fractions of noncondensable gases are examined using scaling and boundary layer techniques, with the aim of defining a criterion for minimum entropy generation rate that is useful in engineering analyses. This process is particularly relevant in humidification-dehumidification desalination systems, where minimizing entropy generation per unit water produced is critical to maximizing system performance. The process is modeled by a consideration of the vapor/gas boundary layer alone, as it is the dominant thermal resistance and, consequently, the largest source of entropy production in many practical condensers with high fractions of noncondensable gases. Most previous studies of condensation have been restricted to a constant wall temperature, but it is shown here that for high concentrations of noncondensable gases, a varying wall temperature greatly reduces total entropy generation rate. Further, it is found that the diffusion of the condensing vapor through the vapor/noncondensable mixture boundary layer is the larger and often dominant mechanism of entropy production in such a condenser. As a result, when seeking to design a unit of desired heat transfer and condensation rates for minimum entropy generation, minimizing the variance in the driving force associated with diffusion yields a closer approximation to the minimum overall entropy generation rate than does equipartition of temperature difference.

Keywords: entropy generation, condensation, noncondensable gas, balancing, heat and mass exchangers, energy efficiency, humidification dehumidification desalination

*Corresponding author
Email address: lienhard@mit.edu (John H. Lienhard V)

Nomenclature

Roman Symbols

B_m	Mass transfer driving force
$\hat{C}$	Dimensionless heat capacity, $c_p M/R$
c	Total molar concentration, kmol/m^3
c_i	Molar concentration of component i, kmol/m^3
c_p	Specific heat at constant pressure, J/kg-K
δ	Boundary layer thickness, m
$\mathscr{D}$	Binary diffusion coefficient, m^2/s
D_{ij}	Multicomponent diffusion coefficient, m^2/s
D_H	Hydraulic diameter, m
D_i^T	Thermal diffusion factor, m^2/s-K
e	Specific internal energy, J/kg
$\mathbf{e_i}$	Unit vector along the ith coordinate
g_i	Partial specific Gibbs free energy of component i, J/kg
$\dot{H}$	Enthalpy rate, W
h	Specific enthalpy, J/kg
h_{conv}	Convective heat transfer coefficient, W/m^2-K
h_i	Partial specific enthalpy of component i, J/kg
HCR	Modified heat capacity rate ratio
$\mathbf{j_i}$	Diffusional flux of component i, kg/m^2-s
$\mathbf{j_s}$	Entropy flux, W/m^2-K
k	Thermal conductivity, W/m-K
Le	Lewis number, Sc/Pr
m_i	Mass fraction of component i
$\dot{m}$	Mass flow rate, kg/s
M_i	Molecular weight of component i, kg/kmol
MR	Mass flow rate ratio
$\mathbf{n}_i$	Net mass flux of component i, kg/m^2-s
Nu	Nusselt number
P	Pressure, Pa
Pr	Prandtl number
Pe	Péclet number
$\mathbf{q}$	Heat flux, W/m^2
R	Universal gas constant, J/kmol-K
Re	Reynolds number

s	Specific entropy, J/kg-K
$\dot{s}'''_{\text{gen}}$	Volumetric rate of entropy generation, W/m^3-K
Sc	Schmidt number
$S'_{\text{gen,HT}}$	Entropy generation rate due to heat transfer per unit tube length, W/m-K
$S'_{\text{gen,MT}}$	Entropy generation rate due to mass transfer per unit tube length, W/m-K
S'_{gen}	Entropy generation rate per unit tube length, W/m-K
S_{gen}	Entropy generation rate, W/K
T	Temperature, K
$\mathbf{u}$	Velocity vector, m/s
u	Axial velocity, m/s
v	Specific volume, kg/m^3
v_r	Radial velocity, m/s
x_i	Mole fraction of component i

Greek Symbols

ϕ	Relative humidity
Φ	Viscous dissipation function
γ	Dimensionless molar concentration
μ	Dynamic viscosity, kg/m-s
ω	Humidity ratio
ρ	Density, kg/m^3
ρ_i	Partial density of component i, kg/m^3
θ	Dimensionless temperature

Subscripts

0	Inlet
av	Average
b	Bulk or mixed-mean
c	Coolant
C	Cold stream
g	Noncondensable gas, air
H	Hot stream
max	Maximum
min	Minimum
v	Water vapor
w	Wall

Superscripts

s	Saturated
$+$	Normalized quantity

1. Introduction

Because a truly reversible process is unachievable in finite time, in good thermal design, one seeks a configuration in which entropy production, or equivalently exergy destruction, is minimized, while meeting practical cost and performance parameters. Several recent studies have highlighted the importance of entropy generation minimization in maximizing the performance of humidification-dehumidification (HDH) desalination systems [1–6]. Of particular relevance here is the conclusion that the greatest source of entropy generation in an HDH system is usually the condenser, or dehumidifier, where large fractions of noncondensable gas (typically 80 to 90%) control the overall heat transfer and condensation rates. This paper is a fundamental study of entropy generation minimization during condensation at high fractions of noncondensable gas.

1.1. Humidification-dehumidification desalination

In order to give the reader context, a brief overview of the HDH system, an intended application of this study, is provided. HDH functions very much like nature's rain cycle. The system consists of three main components: a humidifier, a dehumidifier, and a heater. In the humidifier, warm seawater is sprayed over a packed bed, where dry air evaporates pure water vapor from the falling film of seawater. The warm, moist air then enters a dehumidifier, where the pure vapor condenses on coils cooled by cold, incoming seawater. The seawater is preheated in the process. A water heater between the humidifier and dehumidifier provides the heat input to the system. This particular embodiment of HDH is known as a closed air, open water (CAOW) cycle; there are several others that have been studied in detail [1, 7], but will not be discussed further here.

1.2. Condensation in the presence of noncondensable gases

Much literature has addressed condensation of vapor from mixtures containing noncondensable gases. In particular, the problem of condensing water vapor from an air-steam mixture has received considerable attention. In that process, an air-steam mixture is exposed to a cold surface with a temperature lower than the local saturation temperature. As vapor condenses on the cold surface, the mixture is pulled convectively toward the surface, increasing the concentration of noncondensable gas near the wall. A concentration gradient is established, and the gas diffuses in opposition to the convective motion of the mixture. Temperature and vapor concentration gradients are both significant, and, especially in the case of high fractions of noncondensable gas, both the diffusional and thermal resistances impede the condensation process.

An early attempt at predicting heat transfer coefficients in these mixtures was performed by Colburn [8], who noted when even small amounts of air were present in steam condensers, condensation rates were significantly lower than those predicted by Nusselt theory [9]. A significant body of work was developed by Sparrow and coworkers using laminar boundary layer techniques to evaluate the effects of noncondensable gases, vapor superheating, interfacial resistance, and other phenomena on condensation in external flow in multiple geometries [10–12]. Denny, Mills, and Jusionis [13, 14] studied condensation of a number of species

of vapor in forced, laminar flow using boundary layer equations. The work by Wang and Tu [15] is an early example of an analysis of falling film condensation in a vertical tube with noncondensable gas; the authors found that the effects of noncondensables are more pronounced in enclosures because the concentration of noncondensables increases as condensation proceeds. Various resistance network models have been developed to provide accurate ways to correlate experimental data on in-tube condensation with steam-air, steam-helium, and other mixtures [16–18].

A major application of these studies is in predicting heat transfer coefficients in steam condensers with relatively small amounts of noncondensable gas, such as result from leakage or dissolved gases. Lacking has been the study of condensation in the presence of high concentrations of noncondensable gases in temperature ranges above those normally encountered in HVAC systems (e.g., for which dehumidifiers have been studied in detail). These temperature ranges are of primary interest in HDH desalination systems, for example. In a study that does enter the HDH range, Rao et al. [19] used boundary layer techniques, and their results showed, as expected, that high fractions of noncondensable gas decrease the rate of condensation and heat transfer significantly.

1.3. Balancing and entropy generation minimization in heat exchangers

One approach to entropy generation minimization in a heat exchanger is the technique of balancing. Key to understanding the connection between balancing and entropy generation minimization is the concept of remanent irreversibilities, or "flow imbalances" [20]. Entropy generation minimization by minimizing flow imbalances is in distinct contrast to minimizing entropy generation in heat transfer, say, by minimizing the driving temperature difference across which the heat travels. A simple, well-understood illustration is perhaps the best way to identify this contrast: the balanced, counterflow heat exchanger. When the capacity rates, $\dot{m}c_p$, and the heat transfer coefficients of both streams are approximately constant, the driving temperature difference will be constant along the flow path; this results in a minimization of remanent irreversibilities, even though there still exists a finite temperature difference by which entropy is produced. Indeed, it can be shown analytically that this configuration results in the minimum entropy production for a given set of inlet temperatures and heat exchanger effectiveness [2].

In the case of a heat and mass exchanger (HME), however, $\dot{m}c_p$ does not fully define the axial temperature slope of each stream, owing to latent heat effects, and thus $\dot{m}c_p$ does not define the variation in stream-to-stream driving temperature difference. A more general criterion for minimum entropy production of a fixed duty, fixed volume system undergoing any number of simultaneous transport processes (heat transfer, mass transfer, etc.) is given by Tondeur and Kvaalen [21]. They showed that for a transport process that obeys both the linear relations for entropy generation and Onsager's relations [22, 23] (that is, it obeys the principle of microscopic reversibility, or is not too far removed from thermodynamic equilibrium), the criterion for minimum entropy production when any number of simultaneous transport processes occur is that the local, volumetric rate of entropy generation be constant in space and time. The theoretical result is known as the theorem of minimal dissipation, or equipartition of entropy production (EoEP). When the phenomenological

coefficients–equivalently the heat and mass transfer coefficients–are constant, the equipartition of entropy production is characterized by an equipartition of thermodynamic driving force (EoF).

Johannessen et al. [24] allowed the conjugate heat transfer resistance to vary in a heat transfer process and showed that the equipartition of force is within 1 % of the true minimum, the EoEP, for most practical heat exchangers. Balkan [25] showed that equipartition of temperature difference (EoTD) in a counterflow heat exchanger with a constant overall heat transfer coefficient is a very good representation of the minimum entropy production state.

In the case of a saturated air-steam mixture undergoing a simultaneous, nonzero, heat and mass transfer, however, there cannot exist a process in which the heat and mass transfer driving forces will both be constant over a finite volume. This results from the exponential increase of saturation pressure with interfacial temperature. Saturation temperature and concentration are related monotonically, but not linearly. Hence, the magnitude of the concentration change caused by a given temperature change will be greater if the absolute temperature is greater. This result means that, in contrast to a heat exchanger, entropy generation minimization in an HME fundamentally relies on three parameters: (1) the ratio of the mass flow rates of each stream, (2) the bulk concentration of the diffusing species, and (3) the magnitude of the heat and mass transfer driving forces. As will be shown in the present work, the mean and variance in heat and mass transfer driving forces embody these three criteria completely, unlike the ratio of the minimum to maximum $\dot{m}c_p$.

If, therefore, one cannot achieve the equipartition of all driving forces, it is desirable to identify the dominant source of entropy production and design a flow geometry that results in an equipartition of the driving force associated with that dominant source of entropy generation. In the present analysis, expressions governing entropy production in terms of driving forces and associated fluxes are given, and then applied to a heat and mass exchanger in a general scaling analysis. Next the equations are applied directly in a laminar boundary layer analysis, where several boundary conditions are compared to identify the configuration that results in the true equipartition of entropy production and identify a set of criteria to approximate that minimum. Selected conditions representative of condensers in HDH desalination and HVAC systems are studied. An HDH system has higher rates of mass transfer than contemplated in previous boundary layer analyses of noncondensable gas problems [26], and it involves condensation in the presence of much higher concentrations of noncondensables. However, the majority of the work presented here could be applied to any binary mixture with a single species diffusing out of the control volume of interest.

2. Equations for entropy generation in a boundary layer

Let e be the mass specific internal energy of a mixture consisting of several components i. For a mixture in thermodynamic equilibrium, the canonical relationship states that

$$de = Tds - Pdv + \sum_i g_i dm_i, \tag{1}$$

where T denotes absolute temperature, s the specific entropy, P the pressure, v the specific volume, g_i the partial specific Gibbs energy of the ith species, and m_i the mass fraction of species i. Now consider a perturbation in any number of the thermodynamic properties of the mixture. Assuming local thermodynamic equilibrium, equation (1), may be written it in terms of non-equilibrium gradients as follows. Taking the material derivative, D/Dt, of equation (1) gives

$$\frac{De}{Dt} = T\frac{Ds}{Dt} - P\frac{Dv}{Dt} + \sum_i g_i \frac{Dm_i}{Dt}. \tag{2}$$

The continuity equation, where ρ is the mixture density and $\mathbf{u}$ is the velocity vector, is

$$\frac{D\rho}{Dt} = -\rho \nabla \cdot \mathbf{u}, \tag{3}$$

which may be used to rewrite the derivative in the third term in equation (2):

$$\frac{Dv}{Dt} = -\frac{1}{\rho^2}\frac{D\rho}{Dt} = \frac{1}{\rho}\nabla \cdot \mathbf{u}. \tag{4}$$

The equation of conservation of species is

$$\frac{D\rho_i}{Dt} = -\left(\nabla \cdot \mathbf{j_i} + \rho_i \nabla \cdot \mathbf{u}\right), \tag{5}$$

where ρ_i is the partial density of the ith species and $\mathbf{j_i}$ is a general diffusion vector defined explicitly by equation (10). Using equations (5) and (3), a similar manipulation can be performed to eliminate the fourth term in equation (2):

$$\frac{Dm_i}{Dt} = \frac{D}{Dt}\left(\frac{\rho_i}{\rho}\right) = \rho_i \frac{D}{Dt}\left(\frac{1}{\rho}\right) + \frac{1}{\rho}\frac{D\rho_i}{Dt} = -\frac{1}{\rho}\left(\nabla \cdot \mathbf{j_i}\right). \tag{6}$$

Substituting equations (4) and (6) into equation (2) and rearranging, the time rate change of entropy of the system is

$$\rho\frac{Ds}{Dt} = \frac{1}{T}\left[\rho\frac{De}{Dt} + P\nabla \cdot \mathbf{u} + \sum_i g_i \left(\nabla \cdot \mathbf{j_i}\right)\right]. \tag{7}$$

To write equation (7) entirely in terms of appropriate fluxes and associated driving forces, a thermal energy equation is used to eliminate the material derivative of e. The thermal energy equation for a nonionized gas mixture when forced diffusion is negligible is given by Mills [27] as:

$$\rho\frac{Dh}{Dt} = \frac{DP}{Dt} - \nabla \cdot \mathbf{q} + \sum_i \mathbf{j_i} h_i + \mu\Phi. \tag{8}$$

Here, h is the mixture specific enthalpy, h_i is a partial specific enthalpy, μ is the dynamic viscosity of the mixture, and Φ is the dissipation function. The third term on the right-hand side of equation (8) is enthalpy transport due to diffusion, and vector $\mathbf{q}$ is a generalized heat flux vector comprising ordinary conduction and Dufour conduction:

$$\mathbf{q} = -k\nabla T + RT\sum_i \sum_j \frac{x_i}{M_i}\frac{D_i^T}{D_{ij}}\left(\frac{\mathbf{n}_i}{\rho_i} - \frac{\mathbf{n}_j}{\rho_j}\right), \tag{9}$$

where k is the mixture-based thermal conductivity, R is the universal (molar) gas constant, x_i is the mole fraction of the ith component, M_i is molecular mass, D_i^T is the thermal diffusion factor, D_{ij} is a multicomponent diffusion coefficient, and $\mathbf{n_i}$ is a net mass flux vector. The quantity $\mathbf{j_i}$ is a general diffusion flux vector obtained from the Chapman-Enskog kinetic theory of gases:

$$\mathbf{j_i} = \sum_j m_i m_j D_{ij} \left[\nabla x_j + (x_i - m_j)\nabla \ln P\right] - D_i^T \nabla \ln T. \tag{10}$$

With the aid of equation (3), equation (8) is rewritten in terms of internal energy to obtain a form of the energy equation:

$$\rho \frac{De}{Dt} = -\nabla \cdot \mathbf{q} - P\nabla \cdot \mathbf{u} - \sum_i \nabla \cdot (\mathbf{j_i} h_i) + \mu\Phi. \tag{11}$$

Substituting equation (11) into the modified constitutive relation, equation (7), the final form for the time rate change of entropy is obtained:

$$\rho \frac{Ds}{Dt} = \frac{1}{T}\left\{-\nabla \cdot \mathbf{q} - \sum_i \left[g_i \left(-\nabla \cdot \mathbf{j_i}\right) + \nabla \cdot \mathbf{j_i} h_i\right] + \mu\Phi\right\}. \tag{12}$$

The entropy change may be expressed as the sum of the entropy transferred across the system and the generation of entropy within the system, or

$$\frac{Ds}{Dt} = -\nabla \cdot \mathbf{j_s} + \dot{s}'''_{\text{gen}}.$$

Equation (12) can be written in a form that mirrors the above to isolate the entropy production term:

$$\rho \frac{Ds}{Dt} = \underbrace{-\left[\nabla \cdot \left(\frac{\mathbf{q}}{T}\right) + \sum_i \nabla \cdot \left(\frac{\mathbf{j_i} h_i}{T}\right) - \sum_i \nabla \cdot \left(\frac{\mathbf{j_i} g_i}{T}\right)\right]}_{\text{entropy transferred, } -\nabla \cdot \mathbf{j_s}}$$
$$+ \underbrace{\left[\mathbf{q} \cdot \nabla\left(\frac{1}{T}\right) + \sum_i \mathbf{j_i} h_i \cdot \nabla\left(\frac{1}{T}\right) - \sum_i \mathbf{j_i} \cdot \nabla\left(\frac{g_i}{T}\right) + \frac{\mu\Phi}{T}\right]}_{\text{entropy generated, } \dot{s}'''_{\text{gen}}}.$$

Hence, the local, volumetric rate of entropy production for a mixture undergoing simultaneous heat and mass transfer is:

$$\dot{s}'''_{\text{gen}} = \mathbf{q} \cdot \nabla\left(\frac{1}{T}\right) + \sum_i \mathbf{j_i} h_i \cdot \nabla\left(\frac{1}{T}\right) - \sum_i \mathbf{j_i} \cdot \nabla\left(\frac{g_i}{T}\right) + \frac{\mu\Phi}{T}. \tag{13}$$

Because the desired focus is on the potentially competing effects of simultaneous heat and mass transfer alone, the viscous dissipation term is neglected. It should be noted that this term may contribute significantly to overall entropy production; indeed it may be the dominant term in total entropy generation in fluid undergoing convective heat transfer (see, for example [28]). In the cases considered in the remainder of this analysis, however, entropy generation due to fluid friction will be negligible.

With the aid of a careful consideration of partial specific gibbs energy, [29] showed that equation (13) simplifies to

$$\dot{s}'''_{\text{gen}} = \mathbf{q} \cdot \nabla\left(\frac{1}{T}\right) + \sum_i \left(-\mathbf{j_i} \cdot \frac{1}{T}\nabla g_i|_T\right). \tag{14}$$

Clearly, if $\mathbf{q}$ and $\mathbf{j_i}$ in the above equation are considered solely ordinary conduction and Fickean diffusion, respectively, there is no coupling between heat and mass transfer in the entropy production equation. This conclusion and its significance are described in great detail in [29], but is repeated here because of its particular relevance in the analyses in section 4. For the special case of a binary mixture, equation (14) reduces to

$$\dot{s}'''_{\text{gen}} = k\left(\frac{\nabla T}{T}\right)^2 + \frac{2\rho^2 R D^T}{M_1 M_2 c}\nabla T \nabla m_1 + \frac{\rho^2 R\mathscr{D}}{M_1 M_2 m_1 m_2 c}\left(\nabla m_1\right)^2, \tag{15}$$

where $\mathscr{D}$ is the binary diffusion coefficient.

Next the entropy generation equations are reduced to specific forms that are applied in the subsequent analyses. The air-steam mixture is modeled as ideal with a relatively constant mixture density ρ, or approximately equivalently, constant molar concentration c. In keeping with the condensation literature, subscript v represents the steam, or water vapor, and subscript g represents the air, or noncondensable gas. Only ordinary conduction and Fickean diffusion are considered; other forms of diffusion and conduction are neglected. Conduction and diffusion are assumed to occur in one dimension, y. Then, equation (15) reduces to

$$\dot{s}'''_{\text{gen}} = \frac{k}{T^2}\left(\frac{\partial T}{\partial y}\right)^2 + \frac{\rho^2 R\mathscr{D}}{M_v M_g \rho_v \rho_g c}\left(\frac{\partial \rho_v}{\partial y}\right)^2. \tag{16}$$

On a molar basis, assuming a constant molar concentration, equation (15) may be written, perhaps more neatly, as

$$\dot{s}'''_{\text{gen}} = \frac{k}{T^2}\left(\frac{\partial T}{\partial y}\right)^2 + \frac{\mathscr{D} R c}{c_v c_g}\left(\frac{\partial c_v}{\partial y}\right)^2. \tag{17}$$

Both forms of the entropy generation equation will be used, with mathematical convenience dictating the choice.

3. Scaling analysis

As will be discussed in detail in section 4, the vapor-gas boundary layer is both the dominant resistance in a condenser with high fractions of noncondensable gas and the location of greatest entropy generation rate. The expressions derived in section 2 are first scaled to identify which individual transport process dominates the entropy generation rate under given conditions. Again it is assumed that the transport processes of interest occur only in one dimension, which is representative of the phenomena in many practical heat and mass exchangers.

[Figure 1 about here.]

An arbitrary boundary layer is defined by figure 1. Condensation is assumed only to occur at the surface, where $T = T_{\text{min}}$ and $y = 0$; no mist formation occurs. Again, total molar concentration is assumed to be approximately constant. Vapor diffuses towards the surface and gas diffuses in the opposite direction. Let non-dimensional temperature θ and non-dimensional concentration γ be defined as

$$\theta = \frac{T - T_{\text{min}}}{T_{\text{max}} - T_{\text{min}}}, \tag{18}$$

$$\gamma = \frac{c - c_{\min}}{c_{\max} - c_{\min}}. \tag{19}$$

A nondimensional length scale is defined as the ratio of the coordinate along which the transport occurs to the thickness of the boundary layer corresponding to that specific transported quantity, or $\eta = y/\delta$. The entropy generation equation, (17), can be rewritten using these nondimensional quantities:

$$\dot{s}'''_{\text{gen}} = \underbrace{\frac{k\left(\Delta T\right)^2}{T^2\delta_T^2}\left(\frac{\partial\theta}{\partial\eta}\right)}_{\dot{s}'''_{\text{gen,HT}}} + \underbrace{\frac{\mathscr{D}Rc\left(\Delta c_v\right)^2}{c_v c_g \delta_M^2}\left(\frac{\partial\gamma}{\partial\eta}\right)}_{\dot{s}'''_{\text{gen,MT}}}. \tag{20}$$

Here, δ_T refers to the thermal boundary layer thickness, and δ_M refers to the diffusional boundary layer thickness.

Noting that the two nondimensional gradients will be of order one, the leading coefficients on the gradients indicate the relative contribution of each transport process to total entropy generation. A scaling parameter is then defined as the ratio of entropy generation due to heat transfer to the entropy generation from both heat and mass transfer, or

$$\Psi = \frac{\dot{s}'''_{\text{gen,HT}}}{\dot{s}'''_{\text{gen,HT}} + \dot{s}'''_{\text{gen,MT}}} = \frac{1}{1 + \frac{\dot{s}'''_{\text{gen,MT}}}{\dot{s}'''_{\text{gen,HT}}}}. \tag{21}$$

The parameter Ψ is analogous to the Bejan number Be, which compares entropy generation due to heat transfer and fluid friction in a heat exchanger. Defining Ψ in this manner bounds its value between zero and one. In the present case, when $\Psi = 0$, there is no heat transfer; when $\Psi = 1$, there is no mass transfer. When Ψ is less than 0.1, mass transfer dominates entropy generation and a balanced design should seek to minimize the variance in mass transfer driving force. Conversely, when Ψ is greater than 0.9, heat transfer dominates, and a balanced HME is one with minimal variance in the temperature driving force. In between these two extremes, the effect of one transport process may exceed the other, but no conclusions about which process to balance may be drawn from the scaling analysis alone. In that case, a boundary layer analysis can provide additional insight into configurations that result in the equipartition of entropy production (see section 4).

The parameter Ψ can be written completely in terms of dimensionless parameters, temperatures, and concentrations as

$$\Psi = \left[1 + \frac{\text{Le}}{\hat{C}}\frac{T_{\text{av}}^2}{\left(\Delta T\right)^2}\frac{\left(\Delta c_v\right)^2}{c_{v,\text{av}}c_{g,\text{av}}}\right]^{-1}, \tag{22}$$

where Le is the Lewis number and $\hat{C}$ is a dimensionless heat capacity defined as the ratio of the specific heat of the mixture to the gas constant of the mixture. As the present analysis considers an air-steam mixture, the Prandtl number Pr, the Schmidt number Sc, and Le are all approximately unity. Assuming that the mixture is ideal and is saturated and at atmospheric pressure, Ψ may be evaluated as a function of driving temperature difference at any given average temperature without knowledge of the specific flow geometry.

Plotting Ψ on the ordinate and driving temperature difference on the abscissa for an arbitrary boundary layer in which the mixture is saturated everywhere (figure 2) shows the extent to which mass transfer

controls total entropy generation rate. For the cases considered, mass transfer is the larger (and in some cases, dominant) source of entropy generation in a saturated air-steam mixture undergoing simultaneous heat and mass transfer.

[Figure 2 about here.]

An air-steam mixture that is saturated throughout the boundary layer is representative of various dehumidifiers, including those in a water-heated HDH system as well as household dehumidifiers operating in very humid climates. Particularly in the case of an HDH dehumidifier, which operates at temperatures as high as 70 °C, mass transfer is the dominant source of entropy generation.

As an example, consider a dehumidifier with saturated inlet air at 70 °C and a desired outlet of 50 °C. Assuming the system's driving temperature difference falls between 5 and 15 K, moving up the chart from contour to contour, one can see that Ψ is always much less than unity. Further, Ψ is less than 0.1 for a large portion of the inlet to outlet temperature difference, indicating that mass transfer is the dominant source of entropy production. Thus, to minimize entropy generation in such a dehumidifier, one should seek to minimize the variance in mass transfer driving force.

In the case of an unsaturated boundary layer, mass transfer is not always dominant at the temperatures discussed above. To show this result, plots of Ψ versus driving temperature difference are again generated, where the following assumptions are made in the analysis. In order for the mass transfer to be nonzero, the temperature of the surface on which condensation occurs, $T_{\min}$, must be less than or equal to the dewpoint temperature corresponding to the local drybulb temperature and the local humidity ratio. If no mass transfer has yet occurred, the humidity ratio will be constant throughout the boundary layer. That is, the condition for a nonzero net mass transfer is $T_{\min} \leq T_{\mathrm{dp}}(\eta = 0^+, \omega_0)$. In addition, of course, the concentration gradient that this temperature gradient sets up must be favorable, or $\Delta c = c_{\max} - c_{\min} \geq 0$.

[Figure 3 about here.]

For several values of $T_{\max}$ that bound most dehumidifiers, 15 °C and 70 °C, figure 3 shows the increasing effect of mass transfer as relative humidity $c_{\max}$ is increased. Perhaps unsurprisingly, Ψ rises rapidly to one when the moisture content of the air is not high enough to provide significant condensation: heat transfer dominates entropy generation. However, when the objective is to condense water, or dehumidify, it is desirable to cool the air to a saturated state as quickly as possible, as this provides the maximum rate of condensation. For such a unit, relative humidity will always be unity or near unity over most of the length of the unit, and mass transfer will always be the larger, if not dominant, source of entropy generation.

4. Laminar boundary layer analysis

Next, the equations developed in section 2 are applied directly in a laminar boundary layer analysis. In this section, the model geometry, equations, and code validation are presented first. The section concludes with a discussion of the entropy generation results obtained from the B.L. analysis.

4.1. Model description

Consider the case of in-tube condensation of an air-steam mixture, with geometry and cylindrical coordinates as defined in figure 4. The radial extreme of the control volume is taken at the local interface between the vapor-gas boundary layer and the condensate film. Because the condensate film is very thin relative to the radius R of the pipe, this boundary is set to $r = R$, and is hereafter referred to simply as the wall. The coolant stream is not shown explicitly, but flows countercurrent to the moist air stream in the surrounding annulus.

[Figure 4 about here.]

This control volume is representative of a dehumidifier in an HDH system as a consequence of the high concentrations of air present in the condensing mixture. As a result of high concentrations of noncondensable gas, the dominant resistance between the bulk coolant and the bulk vapor-gas mixture is the vapor-gas boundary layer. Thus, the following approximations can be made. The coolant convective heat transfer coefficient is large, therefore the wall temperature is near the coolant bulk temperature. Second, because a controlling portion of resistance to transport, whether by diffusion or conduction, is in the vapor-gas boundary layer, the entropy generated in the condensate film, tube wall, and coolant boundary layer are taken to be negligible. Hence, entropy generation minimization for an HDH dehumidifier is best approached by a thorough analysis of the mechanisms of entropy production in the vapor-gas boundary layer. Of course, in the case of a low coolant-side heat transfer coefficient, the aforementioned assumptions would not hold.

4.1.1. Transport equations

The appropriate boundary layer equations are now developed. The fluid velocity vector $\mathbf{u}$ is assumed to be two-dimensional, with components in the axial and radial directions: $\mathbf{u} = u\mathbf{e_z} + v_r\mathbf{e_r}$. As previously assumed, the mixture is composed of two ideal gases. Mixture density is assumed to be constant in the radial direction, but varying in the axial direction. The partial densities of each component are permitted to vary in both r and z. Mathematically, $\rho(z) = \rho_v(r, z) + \rho_g(r, z)$. Pressure is assumed to vary only along the length of the pipe z. Thermal diffusion (the Soret effect) and pressure diffusion are neglected so that the diffusion vector contains only the Fickean component. Likewise, only ordinary conduction is considered. In calculating condensation and heat transfer rates, neglecting the Soret and Dufour effects has been shown previously [11] to be acceptable.

The conservation equations for the vapor-gas boundary layer, namely continuity, species, momentum, and energy are, respectively:

$$\frac{u}{\rho}\frac{\partial \rho}{\partial z} + \frac{\partial u}{\partial z} + \frac{1}{r}\frac{\partial}{\partial r}(r v_r) = 0, \tag{23}$$

$$\rho_v \frac{\partial u}{\partial z} + \frac{\rho_v}{r}\frac{\partial}{\partial r}(r v_r) + u\frac{\partial \rho_v}{\partial z} + v_r \frac{\partial \rho_v}{\partial r} = \frac{\mathscr{D}}{r}\left(r\frac{\partial \rho_v}{\partial r}\right), \tag{24}$$

$$\rho u \frac{\partial u}{\partial z} + \rho v_r \frac{\partial u}{\partial r} = -\frac{dP}{dz} + \frac{\mu}{r}\frac{\partial}{\partial r}\left(r\frac{\partial u}{\partial r}\right), \tag{25}$$

$$\rho u c_p \frac{\partial T}{\partial z} + \rho v_r c_p \frac{\partial T}{\partial r} = \frac{k}{r}\frac{\partial}{\partial r}\left(r\frac{\partial T}{\partial r}\right) + \mathscr{D}\frac{\partial \rho_v}{\partial r}\frac{\partial T}{\partial r}(c_{p,v} - c_{p,g}). \tag{26}$$

Properties are assumed constant in r and are evaluated at the mean film temperature, which varies axially. The quantity $\mathscr{D}$ is a binary diffusion coefficient for water in air, and is evaluated using the correlation presented by Marrero and Mason [30]. The specific heat of the mixture is a mass weighted average, $c_p = m_v c_{p,v} + m_g c_{p,g}$. Thermophysical properties implemented here are given by [31] and [32] for water and by [33] for air. In evaluating the mean film temperature, a bulk temperature is required. Here, the bulk temperature is strictly taken as an enthalpy averaged quantity:

$$T_b = \frac{\int_0^R \rho u c_p T\, 2\pi r\, dr}{\int_0^R \rho u c_p\, 2\pi r\, dr}. \tag{27}$$

However, it should be noted that because mixture properties are taken as constant in the boundary layer, neither ρ nor c_p are functions of r, and will thereby cancel from equation (27). The reader should also be aware that this temperature is not physically representative of the adiabatic mixing temperature, as introducing a saturated mixture to an adiabatic mixing chamber might result in condensation.

Psychrometric properties are calculated as follows. The bulk humidity ratio ω_b is the mass of vapor per unit noncondensable gas,

$$\omega_b = \frac{\int_0^R \rho_v u\, 2\pi r\, dr}{\int_0^R (\rho - \rho_v) u\, 2\pi r\, dr}, \tag{28}$$

which is identically equal to the quotient of the bulk partial density of the vapor and the bulk partial density of the noncondensable. To compute relative humidity, the ideal gas relation is used in conjuction with the bulk vapor partial density:

$$\phi = \frac{\rho_v R_v T}{P_v^s(T)}. \tag{29}$$

4.1.2. Boundary conditions

At the inlet of the tube, the velocity and temperature profiles are uniform. Inlet mixture pressure is specified. Relative humidity at the inlet is specified, which allows partial densities for each component to be calculated using the ideal gas relationship. Then, at $z = 0$:

$$u(r,0) = u_0, \tag{30}$$

$$v_r(r,0) = 0, \tag{31}$$

$$T(r,0) = T_0, \tag{32}$$

$$P(0) = P_0, \tag{33}$$

$$\rho_v(r,0) = \frac{\phi_0 P_v^s(T_0)}{R_v T_0}. \tag{34}$$

At all locations beyond the inlet, several boundary conditions are given at the outer extreme of the C.V., where $r = R$. The interface between the vapor-gas boundary layer and the condensate film is impenetrable to the noncondensable gas, so the net flux of the gas component must be zero at that location. The no slip

condition requires that the axial velocity be zero at the wall, assuming that the condensate film velocity is near zero. Because the boundary of the C.V. is at the interface of the vapor-gas boundary layer and the condensate film, where $r = R$, the partial pressure of the vapor must be equal to the saturation pressure corresponding to the local interfacial temperature. From this, the vapor partial density may be calculated. Then, for all $z > 0$:

$$u(R, z) = 0, \tag{35}$$

$$n_g(R, z) = \rho_{g,w} v_r + j_{g,w} = 0, \tag{36}$$

$$T(R, z) = T_w, \tag{37}$$

$$\rho_v(R, z) = \frac{P_v^s(T_w)}{R_v T_w}. \tag{38}$$

The wall temperature, $T_w(z)$, is obtained from an energy balance on the coolant as a function of its mass flow rate, using a prescribed convective heat transfer coefficient:

$$(\dot{m} c_p)_c \frac{dT_{b,c}}{dz} = h_{\text{conv},c} \left(T_w - T_{b,c}\right) 2\pi R. \tag{39}$$

In addition, the conductive heat flux and latent heat of condensation must be absorbed by the coolant:

$$-\left[q_w + n_v(R, z) h_{fg}\right] = h_{\text{conv},c} \left(T_w - T_{b,c}\right). \tag{40}$$

To close the problem, several symmetry conditions are given at the centerline. Namely, the axial velocity profile is smooth, the radial velocity is zero, the radial temperature profile is smooth, and the vapor density profile is smooth. At $r = 0$ for all $z > 0$:

$$\frac{\partial u}{\partial r} = 0, \tag{41}$$

$$v_r = 0, \tag{42}$$

$$\frac{\partial T}{\partial r} = 0, \tag{43}$$

$$\frac{\partial \rho_v}{\partial r} = 0. \tag{44}$$

In summary, the inputs to a given simulation are inlet temperature, pressure, and relative humidity T_0, P_0, and ϕ_0, inlet velocity u_0, coolant inlet bulk temperature, and the mass flow rate ratio MR. The mass flow rate ratio is the quotient of the coolant mass flow rate to the mixture mass flow rate:

$$\text{MR} = \frac{\dot{m}_c}{\int_0^R \rho u \, 2\pi r \, dr} = \frac{\dot{m}_c}{\dot{m}}. \tag{45}$$

4.1.3. Solution method

The conservation equations, (23), (24), (25), (26), are discretized with first order backward difference approximations. Integrals are computed using the trapezoidal rule. The resultant set of algebraic equations is implemented in Engineering Equation Solver (EES) [34], a simultaneous equation solver that uses an

iterative routine to solve sets of coupled non-linear algebraic and/or differential equations. Convergence of a solution is defined when either of two parameters, relative residuals and change in variables, reach predefined values. A relative residual is the absolute value of the difference between the left hand and right hand side of an equation divided by the magnitude of the left hand side of the equation. The term "change in variables" refers to the difference between the value of a variable between the nth and $(n+1)$th iteration. Criteria for relative residuals and change in variables are $< 1.0 \times 10^{-6}$ and $< 1.0 \times 10^{-9}$, respectively, which are the default values in EES. Absent a solution meeting the convergence criteria, EES ceases its solving routine when a predefined number of iterations have been reached or a specified time has elapsed.

4.2. Model and implementation validation

To validate the present model and its numerical implementation, the results of several simulations are compared with well-known results. One heat transfer-only case is considered: constant wall temperature boundary conditions in simultaneously developing, laminar, internal flow. The simulations are also compared to predictions from a low-rate mass transfer approximation. A short discussion of mass transfer rate theory is warranted, as the high concentrations of noncondensable gases inhibit condensation to such a degree that the net mass flux of the vapor through the boundary layer is almost completely diffusive. This is in contrast to condensation in the presence of low fractions of noncondensable gases, where the convective motion of the mixture towards the condensate film is comparatively significant. Though the low-rate approximation is used as a point of comparison, it should be noted that the present model is equally applicable to situations where the mass transfer is high rate.

4.2.1. Comparison with a limiting heat transfer case

The local convective heat transfer coefficient is defined as:

$$h_{\text{conv}} = \frac{k\left(\partial T/\partial r\right)_R}{T_b - T_w}. \tag{46}$$

Defined in this standard way, h_{conv} represents the sensible heat flux only, and it does not include the enthalpy carried by the diffusing vapor. The local Nusselt number is

$$\text{Nu} = \frac{h_{\text{conv}} D_H}{k}. \tag{47}$$

The local Nusselt number varies axially.

Consider a simulation of the present B.L. with the following boundary conditions: $T_0 = 70\,^\circ\text{C}$, $\phi_0 = 0.1$, and a sufficiently high coolant capacity rate such that there is a uniform wall temperature of $T_w = 23\,^\circ\text{C}$. At such low values of inlet humidity, little vapor condensation will occur. In that case, transport through the mixture boundary layer is almost entirely heat transfer, and the results from the simulation may be compared approximately to known cases of heat transfer alone. There exists a well-known series solution for heat transfer in simultaneously developing laminar flow through a duct with circular cross section and a constant wall temperature (see, e.g. [35]). This solution, and the results from several numerical simulations

that model the same configuration are provided as comparison points for model validation. Figure 5, a plot of Nusselt number versus a dimensionless length parameter $z^+ = z/(D_H \mathrm{Pe})$ shows good agreement between the present work and numerical data from Manohar [36], Hornbeck [37], and from Hwang, as reported in [38]. The Churchill and Ozoe [39] curve fit of the series solution, which has an associated error between 6 and 25% is also presented, showing agreement well within those error bounds. As the flow becomes fully developed, $z^+ > 0.037$, the Nusselt number tends to 3.66. The results from the present model trend to within 0.6% of the analytical solution for heat transfer alone.

[Figure 5 about here.]

4.2.2. Comparison with known cases in mass transfer rate theory

With specific boundary conditions, simulation results from the present model may be compared to known cases for pure mass transfer. Mass transfer problems are often subdivided into those termed low rate and those termed high rate. Detailed descriptions of the concepts behind these two categories are described in detail in [40] and [41]; relevant points of each are summarized here for context.

Distinguishing between high- and low-rate mass transfer problems is simplest in terms of the net mass flux of the species,

$$\mathbf{n_i} = \rho_i \mathbf{u_i} + \mathbf{j_i}. \tag{48}$$

The first term on the right hand side of equation (48) represents the convective mass flux of species i; in high-rate mass transfer, this term dominates. In a low-rate mass transfer problem, the second term on the right hand side, the diffusive term, dominates. Because the low-rate model requires that the mass transfer is primarily diffusive, the three conservation equations, species, momentum, and energy, may be solved neglecting the terms that couple the three. Then, the similarity between each equation becomes readily apparent. The Sherwood number is a dimensionless mass transfer coefficient, defined as

$$\mathrm{Sh} = \frac{h_{\mathrm{mass}} D_H}{\mathscr{D}}. \tag{49}$$

The mass transfer coefficient is the quotient of the diffusional mass flux crossing the C.V. boundary and the driving partial density difference, or

$$h_{\mathrm{mass}} = \frac{j_{i,w}}{\Delta \rho_i}. \tag{50}$$

Due to the similarity in the resulting forms of the energy and species equations, it can be seen that in the low-rate approximation, for fully developed, laminar, internal flow, Nu = Sh.

At high relative humidities and temperatures approaching that of vapor saturation at the prescribed pressure (in this case, atmospheric), the concentration of water vapor is high, and that of the noncondensable is low. In that situation, the process would be more representative of the widely-studied problem of pure steam condensation in the presence of a low concentration of noncondensable gas; this is a high-rate mass transfer problem. However, when the noncondensable fraction is high, the net mass flux of vapor is primarily diffusive, and the problem may be solved with reasonable accuracy using the low-rate approximation.

Evaluation of the mass transfer driving force provides an estimate for the upper limit of the low-rate approximation, given by [40] for one species i exiting the control volume boundary as:

$$B_m = \frac{m_{v,b} - m_{v,w}}{1 - m_{v,w}} \lesssim 0.2. \tag{51}$$

For the present problem of an air-steam mixture, an upper bound for B_m occurs when the mixture just begins to condense, $m_{v,b}$ is at a maximum, and $m_{v,w} \simeq 0$. Then, equation (51) reduces to simply $m_{v,b}$. Thus, the low-rate approximation breaks down when the bulk mixture is saturated, has a temperature greater than about 69 °C, and the surface on which condensation occurs is cold and dry, so that $m_{v,w} = 0$. All of the simulations here are within this upper bound, indicating the low-rate approximation is applicable for validation of the model. The departure from Sh = Nu is in part a measure of how good the low-rate approximation is for a given simulation.

Consider the same boundary conditions as given for the heat transfer only case, except with a relative humidity at the inlet of 1 instead of 0.1. Then, the transport through the B.L. is no longer primarily heat transfer, and the problem is one of simultaneous heat and mass transfer. Figures 6a and 6b compare Nu and Sh over the length of the tube for two cases: a high and low inlet temperature, and thus high and low vapor mass fractions. In both cases, the mass flow rate ratio is high, so that the model's wall temperature is held at a constant $T_w = 15\,°\mathrm{C}$. As expected, the greatest discrepancy between Nu and Sh is in the developing region of the high inlet temperature simulation, where B_m is greatest. Clearly, the results given in the present subsection display consistency with accepted solutions to bounding problems.

[Figure 6 about here.]

4.3. Boundary layer model results

Results showing entropy generation rate distribution due to heat and mass transfer in the boundary layer are now discussed. To do so, several parameters are defined. First, a local entropy generation rate, or entropy production rate per unit tube length, is evaluated by integrating equation (16) over the cross-section defined in figure 4:

$$S'_{\mathrm{gen}} = \int_0^R \dot{s}'''_{\mathrm{gen}}\, 2\pi r\, dr = \int_0^R \left[\frac{k}{T^2} \left(\frac{\partial T}{\partial r} \right)^2 + \frac{\rho^2 R \mathscr{D}}{M_v M_g \rho_v \rho_g c} \left(\frac{\partial \rho_v}{\partial r} \right)^2 \right] 2\pi r\, dr. \tag{52}$$

If the integrand is subdivided into entropy generation rate due to heat transfer and that due to mass transfer, entropy production rate per unit tube length due to either phenomenon may be calculated using a similar integration. These two quantities are denoted as $S'_{\mathrm{gen,HT}}$ and $S'_{\mathrm{gen,MT}}$, respectively. Total entropy generation rate for a given configuration is

$$S_{\mathrm{gen}} = \int_0^L \int_0^R \dot{s}'''_{\mathrm{gen}}\, 2\pi r\, dr\, dz. \tag{53}$$

Owing to small variabilities in the numerical implementation, global values of S_{gen} are computed to an accuracy of about 5%.

4.3.1. Balancing and the uniform entropy generation rate

Figure 7 is a plot of local entropy generation rate versus axial position z/L for several MR. For each value of MR, the inlet and outlet air temperatures are fixed; in this case, $T_0 = 40\,^\circ\text{C}$, $\phi_0 = 1$, and the outlet temperature is $10\,^\circ\text{C}$. (These values are more representative of a temperature range encountered in an HVAC system than HDH.) In this manner, the total heat transfer and condensation rates are identical for each curve. Then, by equation (53), the total entropy generation rate for a given mass flow rate ratio is the area under each curve. As the distribution of local entropy generation rate over the tube length becomes more even, the corresponding area under that curve is smaller. This is a verification of the theorem of equipartition of entropy production. For a given heat transfer and diffusion rate, the configuration that results in the lowest entropy generation rate is the one in which the spatial distribution of entropy generation rate is most uniform. Mathematically, this is evaluated by considering the variance in S'_{gen} about a mean value; as this variance approaches a minimum, so does the total entropy generation rate S_{gen} of the system.

[Figure 7 about here.]

The uniform entropy generation rate criteria for minimum entropy generation rate is quite general, and holds irrespective of inlet humidity and temperature. For example, figure 8 shows a set of curves corresponding to an inlet temperature of $T_0 = 70\,^\circ\text{C}$, $\phi_0 = 1$, and an outlet temperature of $40\,^\circ\text{C}$. Although the MR that corresponds to the lowest S_{gen} is not the same, the trend is qualitatively similar; minimum area under the curve corresponds with minimum variance of the curve about its mean value.

[Figure 8 about here.]

In figures 7 and 8, the air inlet and outlet temperatures are fixed. Several combinations of mass flow rate ratio and coolant inlet temperature have then been selected to maintain those air inlet and outlet temperatures, and thus the total heat transfer and diffusion rates. Because the mass flow rate ratio, and thus the enthalpy rate of the coolant, has been varied, figures 7 and 8 and the concept of a uniform entropy generation rate can also be used to explain the concept of balancing from an entropic perspective.

Consider a counterflow tube-in-tube heat exchanger. In such a heat exchanger, it is known that a uniform driving $\Delta T = T_b - T_w$ along the length of the unit leads to a minimum in entropy generation rate for a pair of inlet temperatures and a specified effectiveness. This uniform ΔT is a consequence of balanced capacity rates in each stream, i.e., $(\dot{m}c_p)_{\min}/(\dot{m}c_p)_{\max} = 1$ [2]. This is because the mass flow rate controls the bulk temperature response of a given stream to a given heat transfer, and thus affects the distribution of driving temperature difference ΔT along the length of the tube. The distribution of driving temperature difference is what controls the local distribution of entropy generation rate, and by the theorem of minimal dissipation, the deviation from the minimum global entropy generation rate for the system. From an entropic perspective, therefore, balancing a heat exchanger is fundamentally a manipulation of the capacity rate of a stream to achieve a uniform rate of entropy production. This also implies that, from an entropic perspective, a flow

imbalance, or remanent irreversibility, is nothing other than entropy that is generated due to inequalities in the distribution of the entropy production rate over a finite volume.

For a heat and mass exchanger, however, $\dot{m}$ and c_p both change as the vapor condenses out of the air stream, and $\dot{m}c_p$ does not fully represent the relationship of stream enthalpy rates or heat exchange to temperature and humidity. As a result, $(\dot{m}c_p)_{\min}/(\dot{m}c_p)_{\max} = 1$ does not represent a balanced HME. The alternative concept of a uniform entropy generation rate provides a framework to understand balancing that is considerably more general. That is, if balancing is instead viewed in terms of minimizing the variance in local entropy generation rate, one needs only to understand the dominant sources of entropy generation in any heat and mass exchanger to design for a minimum entropy production rate.

Further, if the configuration that results in the lowest entropy production for any arbitrary diffusion rate and heat transfer rate is the one in which entropy production is most evenly distributed in space, this configuration will be the one that results in the lowest S_{gen} per unit water produced–the normalized entropy generation rate for a desalination system. This conclusion is quite general, and has been found to be valid irrespective of inlet temperature or vapor fraction.

4.3.2. Prediction of the uniform entropy generation rate

The previous subsection established that varying the mass flow rate ratio (or, balancing) is an effective method to create an even entropy generation rate per unit tube length, and thus minimize entropy production rate for the system. However, correlating MR to local entropy production rates at any location in an arbitrary system requires complete knowledge of the temperature and concentration profiles; this is impractical in most engineering design applications. Thus, a criterion that is more easily calculable that approximates the uniform entropy generation rate is desired. An inspection of equation (16) shows the similarity between the expressions for entropy generation rate due to heat transfer across a finite temperature difference and diffusion across a finite concentration difference and it suggests that if a uniform driving temperature difference minimizes entropy generation due to heat transfer, a uniform driving concentration difference will minimize entropy generation due to diffusion.

For example, figure 9a shows S'_{gen} versus z/L, broken down by causal transport process–heat transfer (HT) and mass transfer (MT)–for a relatively low inlet temperature ($T_0 = 35\,^{\circ}\text{C}$). In this case, the particular value of MR has resulted in temperature profile similar to a balanced counterflow heat exchanger, as shown in figure 9b; the driving ΔT is fairly constant along the length of the tube, and, with the exception of a small region near the inlet, the rate of entropy generation due to heat transfer is also spatially uniform. Minimizing the variance in driving temperature difference is thus a good predictor of a minimum variance in entropy generation due to heat transfer. Because temperature and vapor concentration are not linearly related, however, the driving concentration difference $\Delta\rho_v = \rho_{v,b} - \rho_{v,w}$, shown in figure 9c, is not constant in space. The result is a highly nonlinear distribution of entropy generation due to mass transfer, as seen on figure 9a. Further, because diffusion plays a significant role, even at low temperatures, this configuration is not one that minimizes total entropy generation rate.

[Figure 9 about here.]

Clearly, although uniform heat *and* mass transfer driving forces are desirable, it is impossible to achieve both without the ability to alter MR independently at every z. At the high inlet temperatures and vapor fractions encountered in HDH systems, however, mass transfer plays a much more significant role in entropy generation than does heat transfer. Figure 10 shows the entropy generation, temperature, and concentration profiles of such a system; the shape of the mass transfer entropy production curve clearly controls the shape of the sum of the HT and MT curves. (These curves correspond to the dotted line in figure 8). Then, minimizing the variance in driving concentration difference is a good approximation for the minimum entropy generation rate, provided that the resultant temperature profile is not so unbalanced that entropy generation due to heat transfer becomes significant.

[Figure 10 about here.]

The minimum entropy generation rate correlates well with minimum variance in concentration driving difference, particularly in saturated mixtures with temperatures above about 50 °C, which encompasses much of the range of operation of HDH systems. This result can be attributed to the following two factors: (1) Minimum entropy generation due to diffusion results from a uniform driving concentration difference; (2) Diffusion is the largest, and often dominant, source of entropy production in an HDH dehumidifier, so minimizing entropy generation due to diffusion corresponds well to minimizing total entropy generation. This is a key distinction between mechanisms of entropy generation in condensers in HDH systems and those in HVAC systems, which operate at significantly lower temperatures and vapor fractions.

The limit of applicability of the uniform driving $\Delta\rho_v$ as an entropy generation minimization criterion is largely set by the inlet vapor mass fraction. In psychrometric terms, the vapor content of a moist air mixture can be expressed with two parameters: the temperature and a measure of humidity–typically either relative humidity or humidity ratio. It is found that at high temperatures, the relative dominance of diffusion to total entropy production is less sensitive to inlet relative humidity. Take, for example, two cases with $T_0 = 80\,^\circ\mathrm{C}$ and inlet relative humidity of 1 and 0.2. Even at a low relative humidity, entropy generation due to mass transfer is quite large. In contrast, at low inlet temperatures, the relative dominance of diffusion to total entropy generation rate is significantly more sensitive to relative humidity.

Inlet relative humidity is a poor indicator of vapor content in moist air condensers that operate over large temperature ranges. In comparison to HVAC systems, the high mixture temperature is high enough to allow for high mass fractions of vapor even at low relative humidities, and in evaluating relative rates of entropy generation, it is the mass fraction (or concentration) of the vapor at the inlet that is important. Thus, the humidity ratio is more predictive of the dominance of entropy generation due to mass transfer.

Thus far, discussion has been restricted to a consideration of flows that are thermally and hydraulically fully developed for a majority of the length of the tube. The effect of varying heat and mass transfer coefficients on the prediction of the uniform entropy generation rate is now considered. Several simulations

were performed in which the flow was neither hydraulically nor thermally fully developed for a majority of the length. In these cases, minimum entropy generation rate still corresponded well with minimum variance in local entropy generation rate. However, the simulations were not characterized by a constant driving temperature or concentration difference. For example, compare figures 11 and 12. In figure 11, as the flow reaches the fully developed condition, the driving potentials become approximately constant in space, and the spatial distribution of entropy generation rate becomes flat. This is in contrast to figure 12, in which the rate of entropy generation increases noticeably as the flow becomes fully developed. Perhaps counterintuitively, the configuration with nonuniform driving $\Delta\rho_v$ (shown in figure 12) that results in the lower overall S_{gen}.

[Figure 11 about here.]

[Figure 12 about here.]

The discrepancy resulting from varying heat and mass transfer coefficients is because the spatial variance in the driving force is greater in the presence of developing boundary layers.

The final key factor that distinguishes balancing in moist air condensers from that in pure heat exchangers is the effect of saturation line curvature on a stream's enthalpy rate. When vapor fractions are high, it has been shown that without the ability to change the MR at every z, a perfectly uniform distribution of S'_{gen} is difficult to achieve; the variance may be minimized, but there still exists curvature in the plots of S'_{gen} versus z/L. Further, the curvature is visually greater at higher temperatures (compare the dashed curves in figures 7 and 8). This is a result of the exponential nature of the saturation curve.

As a conceptual example, consider an arbitrary position z in the tube; if the bulk is saturated and condensation occurs, both the wall and bulk states are saturated, and these may be plotted on the saturation curve, as shown in figure 13. At another location $z + \Delta z$, the change in position of both of these points is entirely determined by the enthalpy rate of the stream and the transport coefficients. At the low end of the saturation curve, the difference in curvature between the wall and bulk states is smaller than at the higher end, and thus a condenser operating at these temperatures is more easily balanced. Further, if the heat transfer coefficients are such that the driving ΔT and $\Delta\rho_v$ are small, both points on figure 13 will experience locally similar curvatures, and the axial concentration and temperature slopes at the wall and in the bulk will tend not to diverge.

[Figure 13 about here.]

4.3.3. Summary of entropy generation results

As discussed previously, a particular set of curves such as those shown in figure 9a was obtained by selecting fixing an air inlet and outlet temperature, and then varying the coolant inlet temperature and mass flow rate. In this manner, a single set of data represents a single overall heat transfer and condensation rate, and dimensional values of entropy generation rate may be compared to identify a minimum. However, without normalization, entropy generation rates may not be compared between sets of data. As detailed

in section 4.3.1, because neither the mixture mass flow rate nor its specific heat are constant, the product of mass flow rate and specific heat is not an appropriate normalization parameter for entropy generation. Thus, in order to compare entropy generation rates between sets, a normalized total entropy generation rate is defined as

$$S^{+}_{\mathrm{gen}} = \frac{S_{\mathrm{gen},i} - S_{\mathrm{gen,min},i}}{S_{\mathrm{gen,max},i} - S_{\mathrm{gen,min},i}}, \tag{54}$$

where the subscript i indicates that the minimum and maximum entropy generation rates are local to a single overall heat transfer and condensation rate; i.e., the minimum and maximum values of S_{gen} for a given inlet and outlet air temperature and vapor fraction. Normalized standard deviation (the square root of the variance) in entropy generation rate per unit tube length is defined in a similar manner, viz.:

$$\sigma^{+} = \frac{\sigma(S'_{\mathrm{gen},i}) - \left[\sigma(S'_{\mathrm{gen},i})\right]_{\mathrm{min}}}{\left[\sigma(S'_{\mathrm{gen},i})\right]_{\mathrm{max}} - \left[\sigma(S'_{\mathrm{gen},i})\right]_{\mathrm{min}}}. \tag{55}$$

Plotting equation (54) on the ordinate and (55) on the abscissa for several inlet to outlet temperature ranges and MR, as shown in figure 14, provides a succinct verification of the optimality criterion originally proposed by Tondeur and Kvaalen [21]. (The data range from a high inlet temperature of 70 °C to a low outlet temperature of 10 °C.) As the distribution of S'_{gen} becomes more uniform, overall S_{gen} decreases, irrespective of inlet conditions and variation in heat and mass transfer coefficients.

[Figure 14 about here.]

Defining a normalized standard deviation in driving temperature difference in a manner analogous to that for local entropy generation rate, (55), allows total entropy generation rate to be compared to local variations in driving temperature difference. It can be seen in figure 15 that a constant driving temperature difference does not always correspond to a minimum entropy generation rate, as would be the case, approximately, in a heat exchanger. A plot of entropy generation rate versus a normalized standard deviation in driving partial density difference in figure 16, however, displays a more similar correlation to figure 14. The minimum entropy generation rate corresponds better with the minimum in driving partial density difference because the entropy generation rate is largely controlled by diffusion at the configurations presented.

[Figure 15 about here.]

[Figure 16 about here.]

4.4. Comparison of B.L. results with control volume methods of heat and mass exchanger entropy generation minimization

As discussed previously, in a heat exchanger, when the capacity rate ratio (the ratio of minimum to maximum $\dot{m}c_p$) is unity, entropy generation is minimized. However, because the product $\dot{m}c_p$ is neither the total derivative $d\dot{H}/dT$ nor constant for an HME, Narayan et al. [2] have proposed a modified heat capacity

rate ratio. The modified heat capacity rate ratio HCR, is defined as the ratio of maximum enthalpy rate of the cold stream to that of the hot stream:

$$\mathrm{HCR} = \frac{\Delta \dot{H}_{\max,C}}{\Delta \dot{H}_{\max,H}}. \tag{56}$$

Analogous to the balanced counterflow heat exchanger, those authors have shown analytically that for fixed inlet temperatures and effectiveness, normalized entropy generation for the HME is minimized when HCR is one. In the case of a condenser, the expression for HCR is

$$\mathrm{HCR} = \frac{\dot{m}_c c_{p,c}(T_0 - T_{b,c,\mathrm{in}})}{\dot{m}(h_{b,\mathrm{in}} - h_{b,\mathrm{out}}^{\mathrm{ideal}}) - \int_0^L n_{v,w} h_{v,w}\, 2\pi R\, dz}, \tag{57}$$

where the superscript ideal indicates that that particular enthalpy should be evaluated at the coolant inlet temperature. The maximum change in enthalpy rate is essentially defined by a temperature pinch; the lowest outlet temperature the air can reach is the coolant inlet temperature. Likewise, the highest temperature the water can reach is the air inlet temperature.

Using equation (57), HCR can easily be calculated for the present configurations. It was found that the configurations that resulted in the most even distributions of S'_{gen} also yielded an HCR of approximately unity. Referring again to figures 7 and 8, it can be seen that the value of HCR closest to one corresponds with the most even spatial distribution of S'_{gen}. An HCR of approximately one is consistent with the uniform entropy generation rate criterion for minimum global entropy generation rate.

5. Conclusions

Mechanisms of entropy generation in condensers with high fractions of noncondensable gas have been examined with the aim of providing a set of criteria useful in engineering analyses for designing toward a minimum entropy production rate. In the present analysis, the following major conclusions have been demonstrated:

1. From an entropic perspective, balancing for any heat and mass exchanger is fundamentally the manipulation of (1) the enthalpy rate of a stream and (2) the heat and mass transfer coefficients of a stream in order to create a spatially even distribution of entropy generation rate.
2. For any set of dehumidifiers of a given heat transfer rate, condensation rate, and size, entropy generation approaches a minimum when the entropy generation rate approaches uniformity in space, or when the variance in the entropy generation rate is minimized. This is a verification of the theorem of equipartition of entropy production (EoEP).
3. For any set of dehumidifiers of a given heat transfer rate, condensation rate, and size, the entropy generation due to heat transfer approaches an approximate minimum when the variance in driving temperature difference is minimized. Likewise, entropy generation due to diffusion approaches an approximate minimum when the variance in driving vapor partial density (or concentration) difference is minimized. However, a configuration that minimizes both simultaneously is unachievable except in the case of very small heat and mass transfer driving forces.

4. For many practical condensers with high fractions of noncondensable gas, the coolant thermal resistance and bulk-to-wall temperature difference is low, and the dominant source of entropy generation is in the vapor/gas boundary layer. This result means that any attempt at entropy generation minimization should be focused on the vapor/gas B.L. Further, it has been shown that for an air/steam mixture, the physical mechanism that has the largest relative contribution to entropy generation is diffusion.
5. As a result of the three above items, a good approximation for the configuration that minimizes entropy generation rate in condensers with high concentrations of noncondensable gases is a constant driving concentration difference.
6. At lower temperatures and low driving values of heat and mass transfer driving forces, temperature- and diffusion-balanced configurations have fairly insignificant differences in total entropy generation rate. This is due to the exponential curvature of the vapor pressure line.
7. When developing flow effects are significant, or spatial variations in heat and mass transfer coefficients are significant, minimizing the variance in driving concentration difference corresponds to the minimum entropy production rate, but it does not correspond to a constant value of driving concentration difference.

Acknowledgements

The authors would like to thank the King Fahd University of Petroleum and Minerals for funding the research reported in this paper through the Center for Clean Water and Clean Energy at MIT and KFUPM. Gratitude is also extended to the MIT Energy Initiative and its partner Eni, who supported the present work through a fellowship granted to the first author.

[1] G. P. Narayan, M. H. Sharqawy, and J. H. Lienhard V, "Thermodynamic analysis of humidification dehumidification desalination cycles," *Desalination and Water Treatment*, vol. 16, no. 1-3, pp. 339–353, 2010.

[2] G. P. Narayan, J. H. Lienhard V, and S. M. Zubair, "Entropy generation minimization of combined heat and mass transfer devices," *International Journal of Thermal Sciences*, vol. 49, no. 10, pp. 2057 – 2066, 2010.

[3] G. P. Narayan, K. H. Mistry, M. H. Sharqawy, S. M. Zubair, and J. H. Lienhard V, "Energy effectiveness of simultaneous heat and mass exchange devices," *Frontiers in Heat and Mass Transfer*, vol. 1, no. 2, pp. 1–13, 2010.

[4] K. H. Mistry, J. H. Lienhard V, and S. M. Zubair, "Effect of entropy generation on the performance of humidification-dehumidification desalination cycles," *International Journal of Thermal Sciences*, vol. 49, no. 9, pp. 1837 – 1847, 2010.

[5] K. H. Mistry, A. Mitsos, and J. H. Lienhard V, "Optimal operating conditions and configurations for humidification-dehumidification desalination cycles," *International Journal of Thermal Sciences*, vol. 50, no. 5, pp. 779 – 789, 2011.

[6] K. H. Mistry, R. K. McGovern, G. P. Thiel, E. K. Summers, S. M. Zubair, and J. H. Lienhard V, "Entropy generation analysis of desalination technologies," *Entropy*, vol. 13, no. 10, pp. 1829–1864, 2011.

[7] G. P. Narayan, M. H. Sharqawy, E. K. Summers, J. H. Lienhard V, S. M. Zubair, and M. A. Antar, "The potential of solar-driven humidification-dehumidification desalination for small-scale decentralized water production," *Renewable and Sustainable Energy Reviews*, vol. 14, no. 4, pp. 1187–1201, 2010.

[8] A. P. Colburn and O. A. Hougen, "Design of cooler condensers for mixtures of vapors with noncondensing gases," *Industrial and Engineering Chemistry*, vol. 26, pp. 1178–1182, November 1934.

[9] W. Nußelt, "Die oberflächenkondensation des wasserdampfes," *Zeitschrift des Vereins Deutscher Ingenieure*, vol. 60, pp. 541–546, 1916.

[10] E. M. Sparrow and E. Eckert, "Effects of superheated vapor and noncondensable gases on laminar film condensation," *AIChE Journal*, vol. 7, no. 3, pp. 473–477, 1961.

[11] W. J. Minkowycz and E. M. Sparrow, "Condensation heat transfer in the presence of noncondensables, interfacial resistance, superheating, variable properties, and diffusion," *International Journal of Heat and Mass Transfer*, vol. 9, no. 10, pp. 1125–1144, 1966.

[12] E. M. Sparrow, W. J. Minkowycz, and M. Saddy, "Forced convection condensation in the presence of noncondensables and interfacial resistance," *International Journal of Heat and Mass Transfer*, vol. 10, no. 12, pp. 1829 – 1845, 1967.

[13] V. E. Denny, A. F. Mills, and V. J. Jusionis, "Laminar film condensation from a steam-air mixture undergoing forced flow down a vertical surface," *Journal of Heat Transfer*, vol. 93, no. 3, pp. 297–304, 1971.

[14] V. E. Denny and V. J. Jusionis, "Effects of noncondensable gas and forced flow on laminar film condensation," *International Journal of Heat and Mass Transfer*, vol. 15, no. 2, pp. 315 – 326, 1972.

[15] C.-Y. Wang and C.-J. Tu, "Effects of non-condensable gas on laminar film condensation in a vertical tube," *International Journal of Heat and Mass Transfer*, vol. 31, no. 11, pp. 2339 – 2345, 1988.

[16] T. Kageyama, P. F. Peterson, and V. E. Schrock, "Diffusion layer modeling for condensation in vertical tubes with noncondensable gases," *Nuclear Engineering and Design*, vol. 141, no. 1-2, pp. 289 – 302, 1993.

[17] H. A. Hasanein, M. S. Kazimi, and M. W. Golay, "Forced convection in-tube steam condensation in the presence of noncondensable gases," *International Journal of Heat and Mass Transfer*, vol. 39, no. 13, pp. 2625 – 2639, 1996.

[18] S. Z. Kuhn, V. E. Schrock, and P. F. Peterson, "An investigation of condensation from steam-gas mixtures flowing downward inside a vertical tube," *Nuclear Engineering and Design*, vol. 177, no. 1-3, pp. 53 – 69, 1997.

[19] V. D. Rao, V. M. Krishna, K. V. Sharma, and P. M. Rao, "Convective condensation of vapor in the presence of a non-condensable gas of high concentration in laminar flow in a vertical pipe," *International Journal of Heat and Mass Transfer*, vol. 51, no. 25-26, pp. 6090 – 6101, 2008.

[20] A. Bejan, *Advanced engineering thermodynamics*. John Wiley & Sons, 2006.

[21] D. Tondeur and E. Kvaalen, "Equipartition of entropy production. an optimality criterion for transfer and separation processes," *Industrial & Engineering Chemistry Research*, vol. 26, no. 1, pp. 50–56, 1987.

[22] L. Onsager, "Reciprocal relations in irreversible processes. i.," *Physical Review*, vol. 37, pp. 405–426, Feb 1931.

[23] L. Onsager, "Reciprocal relations in irreversible processes. ii.," *Physical Review*, vol. 38, pp. 2265–2279, Dec 1931.

[24] E. Johannessen, L. Nummedal, and S. Kjelstrup, "Minimizing the entropy production in heat exchange," *International Journal of Heat and Mass Transfer*, vol. 45, no. 13, pp. 2649 – 2654, 2002.

[25] F. Balkan, "Comparison of entropy minimization principles in heat exchange and a short-cut principle: Eotd," *International Journal of Energy Research*, vol. 27, no. 11, pp. 1003–1014, 2003.

[26] J. Y. San, W. M. Worek, and Z. Lavan, "Entropy generation in combined heat and mass transfer," *International Journal of Heat and Mass Transfer*, vol. 30, no. 7, pp. 1359 – 1369, 1987.

[27] A. F. Mills, "The use of the diffusion velocity in conservation equations for multicomponent gas mixtures," *International Journal of Heat and Mass Transfer*, vol. 41, no. 13, pp. 1955 – 1968, 1998.

[28] A. Bejan, "General criterion for rating heat-exchanger performance," *International Journal of Heat and Mass Transfer*, vol. 21, no. 5, pp. 655 – 658, 1978.

[29] C. G. Carrington and Z. F. Sun, "Second law analysis of combined heat and mass transfer phenomena," *International Journal of Heat and Mass Transfer*, vol. 34, no. 11, pp. 2767 – 2773, 1991.

[30] T. R. Marrero and E. A. Mason, "Gaseous diffusion coefficients," *Journal of Physical and Chemical Reference Data*, vol. 1, no. 1, pp. 3–118, 1972.

[31] W. Wagner and A. Pruß, "The IAPWS formulation 1995 for the thermodynamic properties of ordinary water substance for general and scientific use," *Journal of Physical and Chemical Reference Data*, vol. 31, no. 2, pp. 387–535, 2002.

[32] J. Kestin, J. V. Sengers, B. Kamgar-Parsi, and J. M. H. Levelt Sengers, "Thermophysical properties of fluid H_2O," *Journal of Physical and Chemical Reference Data*, vol. 13, no. 1, pp. 175–183, 1984.

[33] E. W. Lemmon, R. T. Jacobsen, S. G. Penoncello, and D. G. Friend, "Thermodynamic properties of air and mixtures of nitrogen, argon, and oxygen from 60 to 2000 K at pressures to 2000 MPa," *Journal of Physical and Chemical Reference Data*, vol. 29, no. 3, pp. 331–385, 2000.

[34] S. A. Klein, *Engineering Equation Solver*. F-Chart Software, LLC.

[35] J. R. Sellars, M. Tribus, and J. S. Klein, "Heat transfer to laminar flow in a round tube or flat conduit– The Graetz problem extended," *Transactions of the American Society of Mechanical Engineers*, vol. 78, pp. 441–448, 1956.

[36] R. Manohar, "Analysis of laminar-flow heat transfer in the entrance region of circular tubes," *International Journal of Heat and Mass Transfer*, vol. 12, no. 1, pp. 15 – 22, 1969.

[37] R. W. Hornbeck, "An all-numerical method for heat transfer in the inlet of a tube," No. 65-WA/HT-36, 1965.

[38] R. K. Shah and A. L. London, *Advances in Heat Transfer Supplement 1: Laminar Flow Forced Convection In Ducts*. Academic Press, Inc., 1978.

[39] S. W. Churchill and H. Ozoe, "Correlations for laminar forced convection in flow over an isothermal flat plate and in developing and fully developed flow in an isothermal tube," *Journal of Heat Transfer*, vol. 95, no. 3, pp. 416–419, 1973.

[40] J. H. Lienhard IV and J. H. Lienhard V, *A Heat Transfer Textbook*. Dover Publications, Inc., 4th ed., 2011.

[41] A. F. Mills, *Mass Transfer*. Prentice Hall, 1st ed., May 2001.

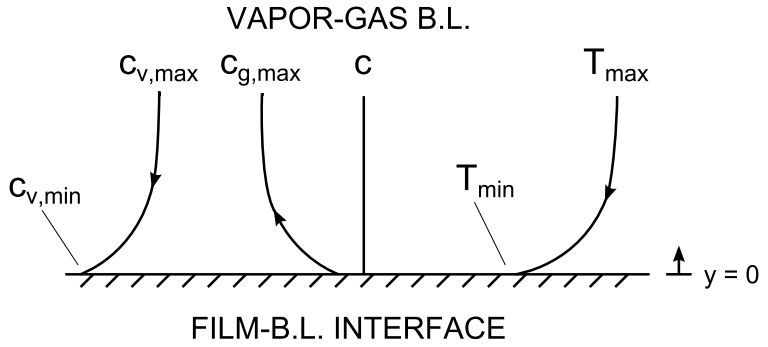

Figure 1: Arbitrary boundary layer through which 1-D conduction and diffusion occurs. The total molar concentration c is assumed constant through the B.L.

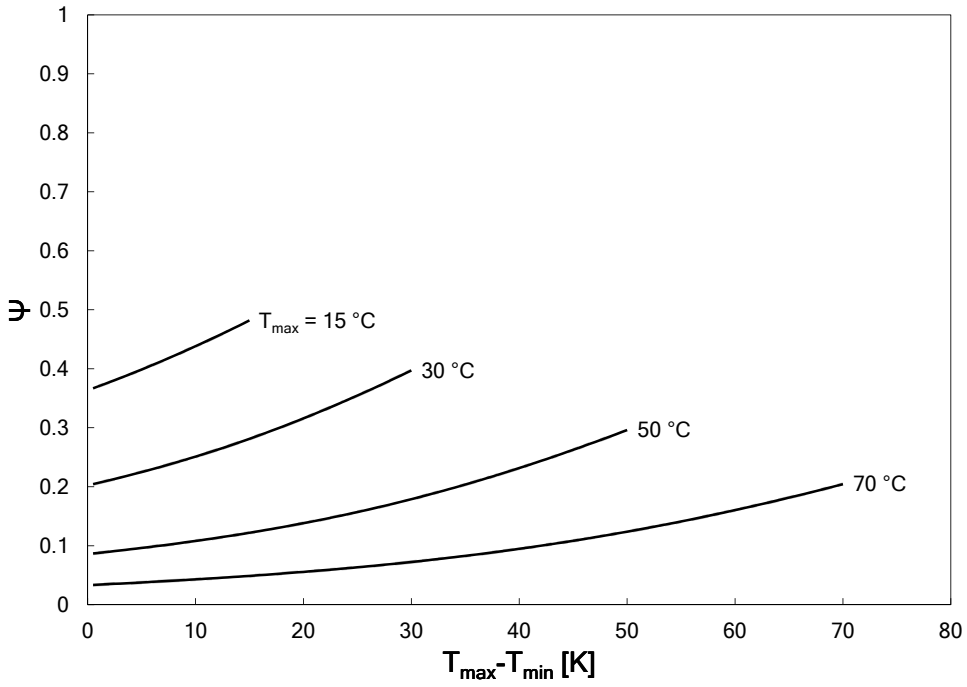

Figure 2: Entropy generation scaling parameter Ψ versus maximum temperature difference for a saturated boundary layer: diffusion is the dominant source of entropy production for the temperature ranges and driving temperature differences encountered in HDH systems.

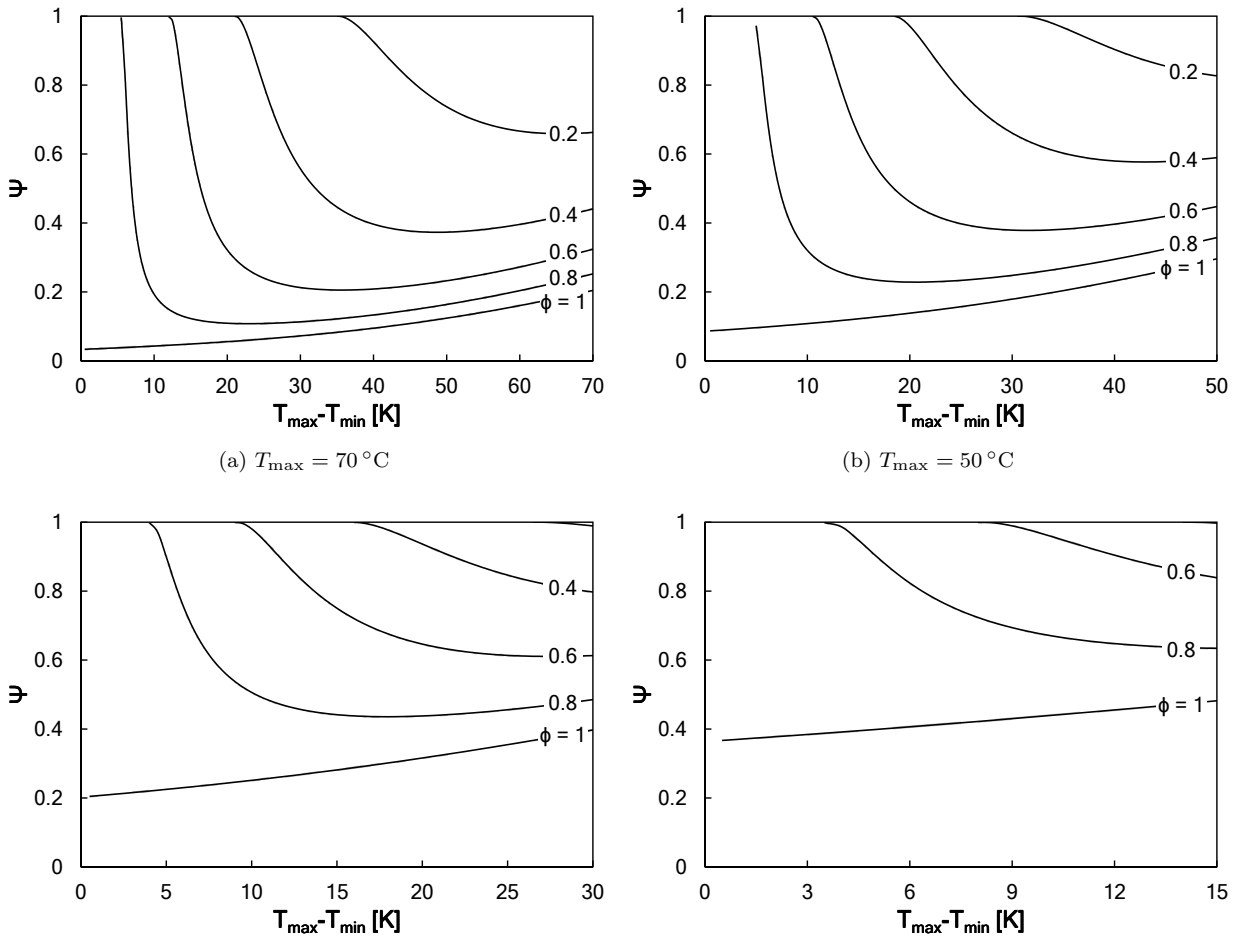

(a) $T_{\max} = 70\,^{\circ}\mathrm{C}$

(b) $T_{\max} = 50\,^{\circ}\mathrm{C}$

(c) $T_{\max} = 30\,^{\circ}\mathrm{C}$

(d) $T_{\max} = 15\,^{\circ}\mathrm{C}$

Figure 3: Entropy production scaling parameter vs. driving temperature difference at specified $T_{\max}$ where $c_{\min}$ corresponds to the saturated concentration at the local T, and contours indicate relative humidity at the location where $c = c_{\max}$.

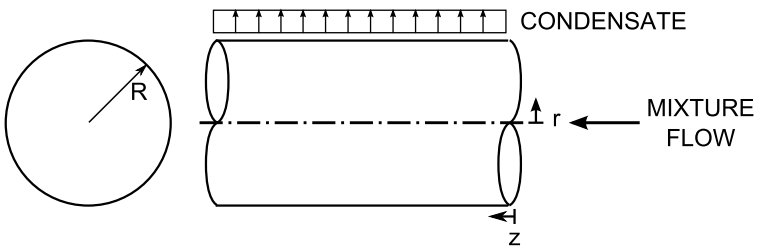

Figure 4: In-tube condenser geometry and coordinate system. The coolant (not shown) flows countercurrent to the air-steam mixture in a surrounding annulus.

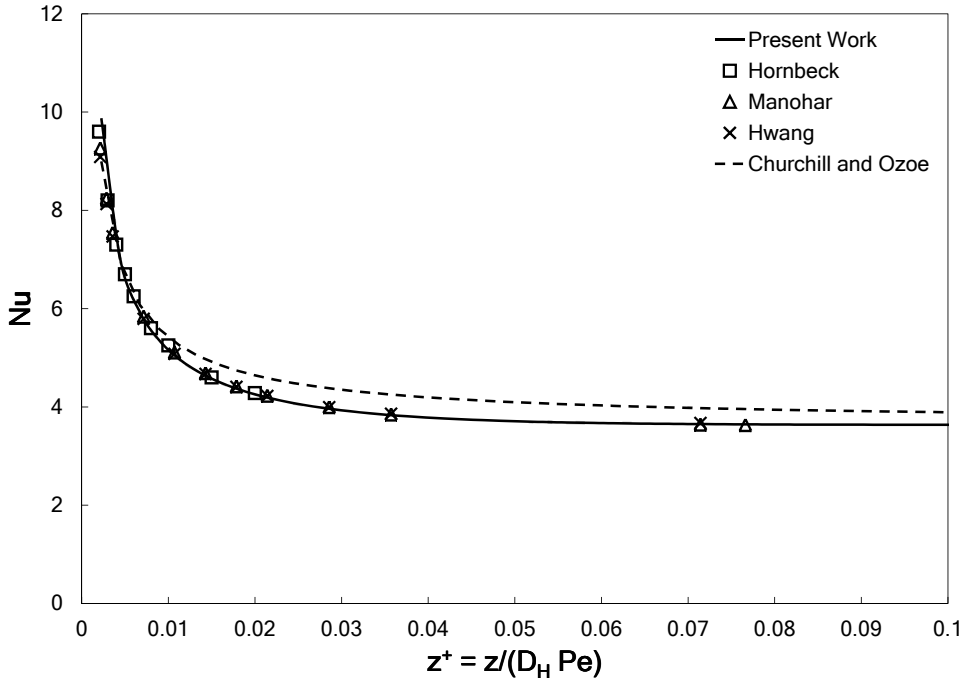

Figure 5: A plot of Nusselt number versus dimensionless length for a low inlet relative humidity and a constant wall temperature validates numerics of the present work.

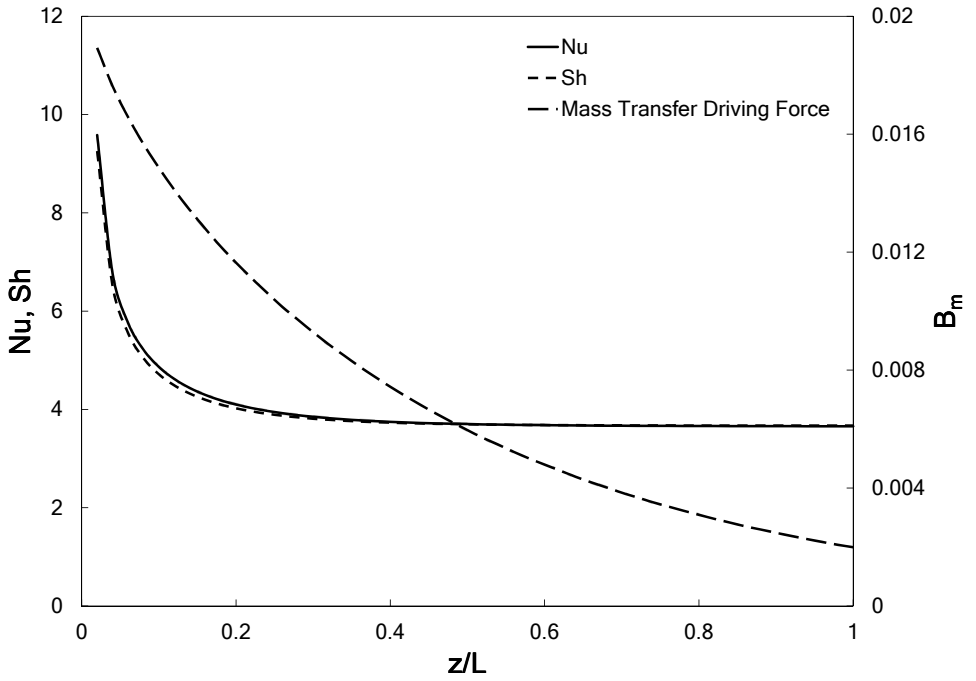

(a) Low inlet temperature and vapor fraction

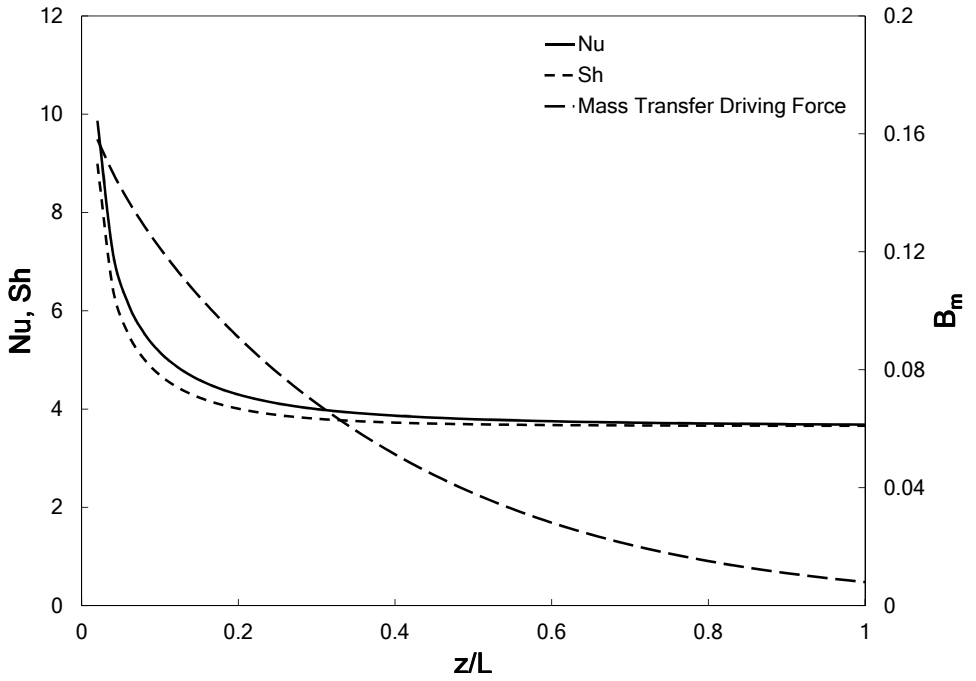

(b) High inlet temperature and vapor fraction

Figure 6: Nu and Sh versus length for low (a) and high (b) inlet temperatures and vapor fractions. In both bounding cases, Nu and Sh parallel one another outside the region where developing flow effects are significant.

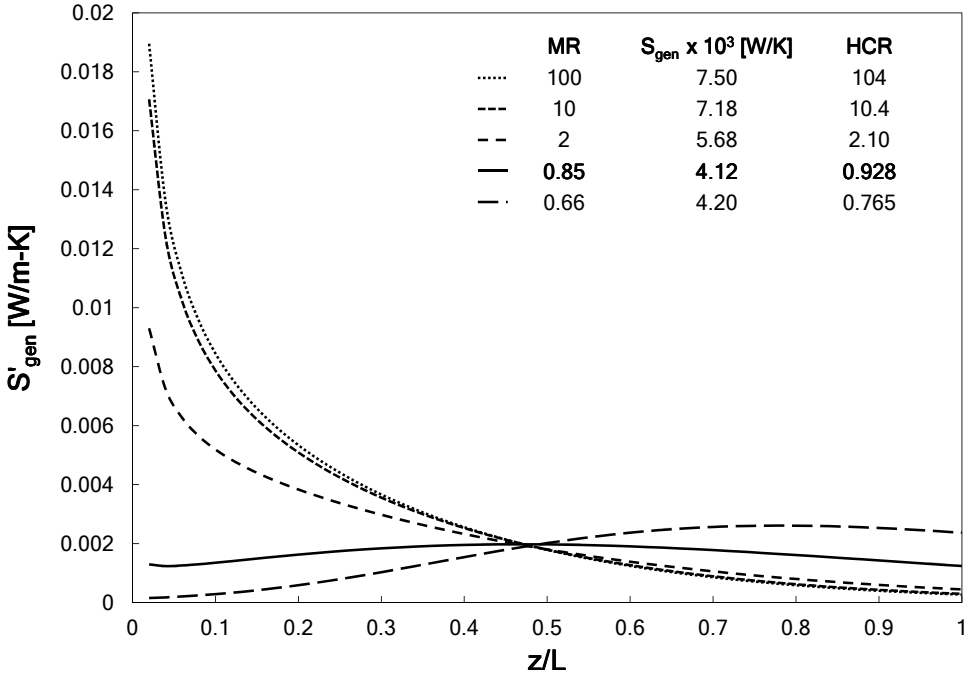

Figure 7: Minimizing the variance in local entropy generation rate leads to a global minimum in entropy production rate: curves with the most even distribution of S'_{gen} have the smallest area under the curve. The solid curve indicates the lowest total entropy production rate.

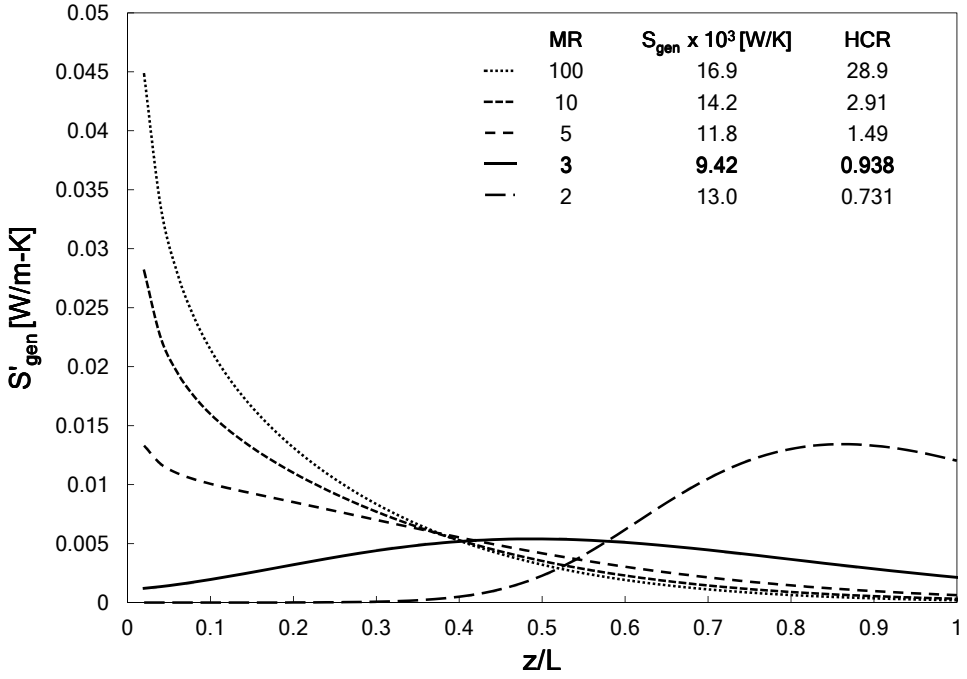

Figure 8: Minimizing the variance in local entropy generation rate leads to a global minimum in entropy production rate: curves with the most even distribution of S'_{gen} have the smallest area under the curve. The solid curve indicates the lowest total entropy production rate.

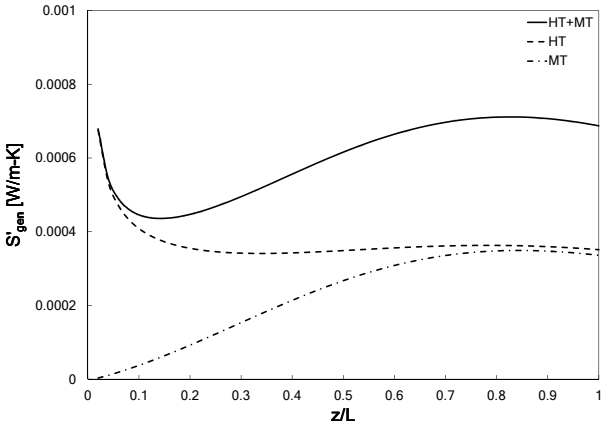

(a) Distribution of entropy production rate.

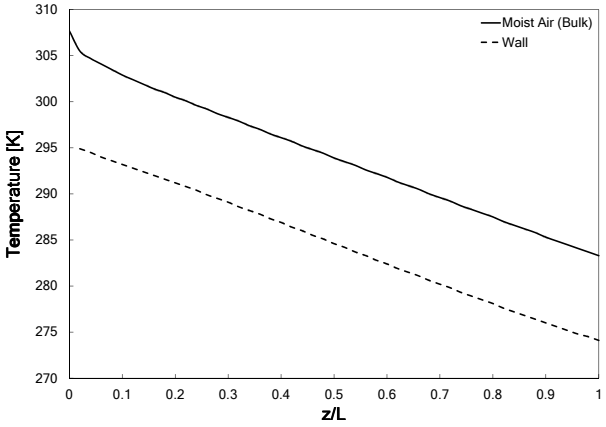

(b) Temperature profile.

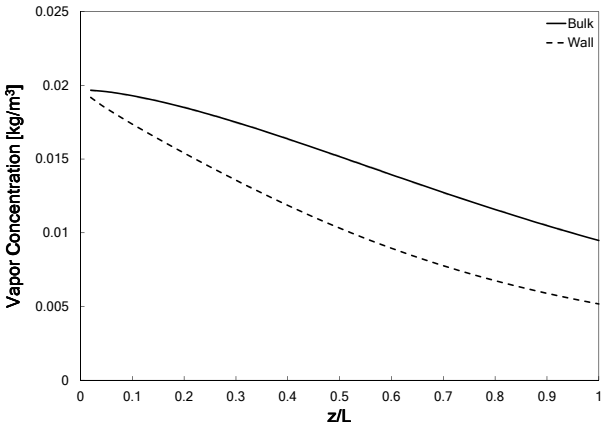

(c) Vapor concentration profile.

Figure 9: Entropy generation, temperature, and concentration profiles in a temperature-balanced system with low inlet vapor fraction.

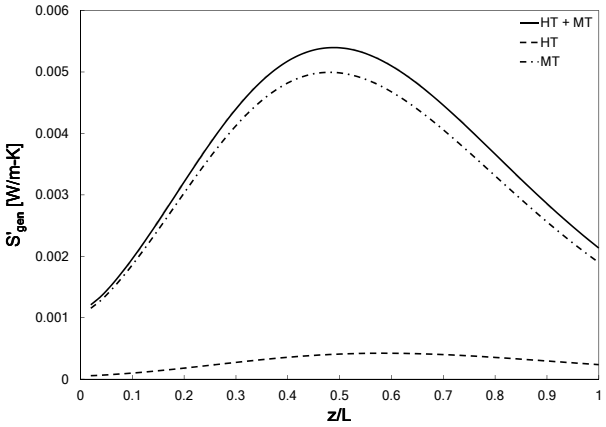

(a) Distribution of entropy production rate.

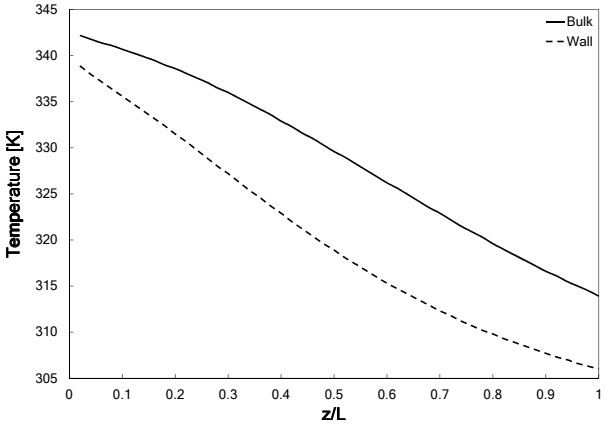

(b) Temperature profile.

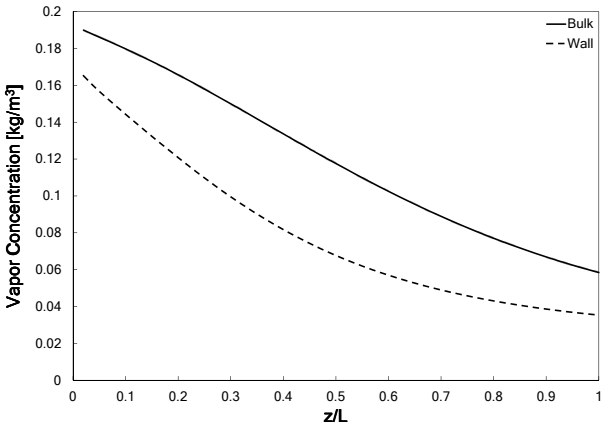

(c) Vapor partial density profile.

Figure 10: Entropy generation, temperature, and concentration profiles in a balanced system with high inlet vapor fraction.

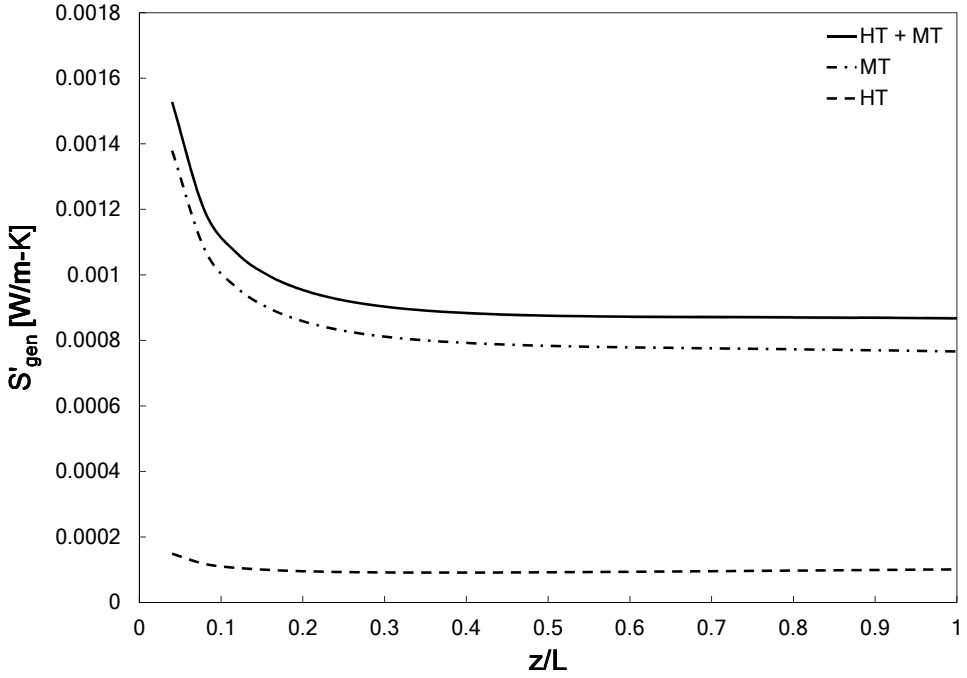

Figure 11: Entropy generation profile for a constant driving $\Delta\rho_v$ in the fully developed region.

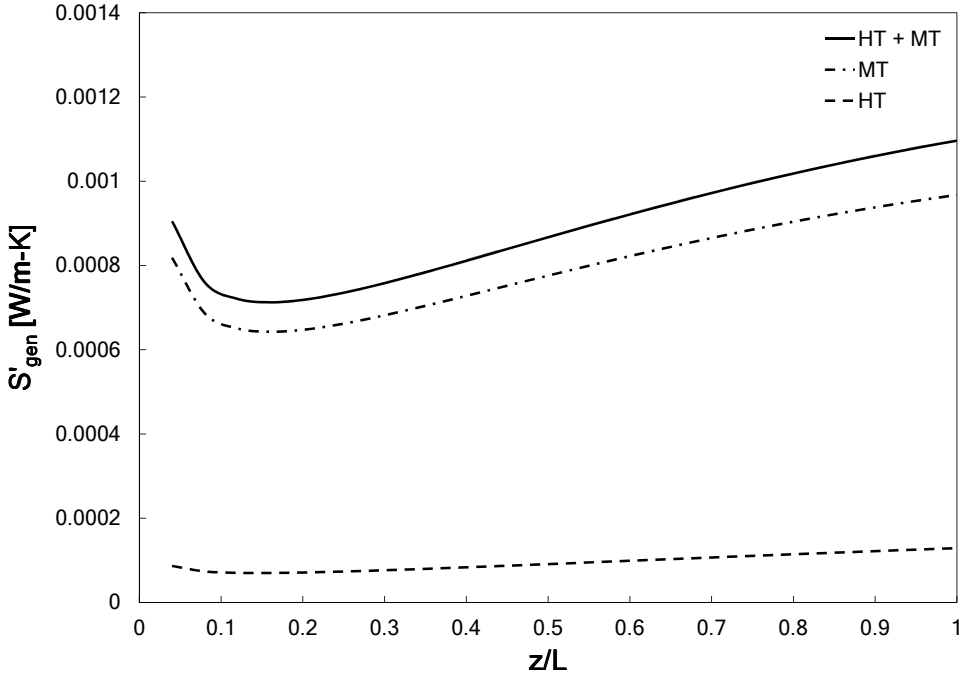

Figure 12: Entropy generation profile for a minimum variance in driving $\Delta\rho_v$ across the entire length.

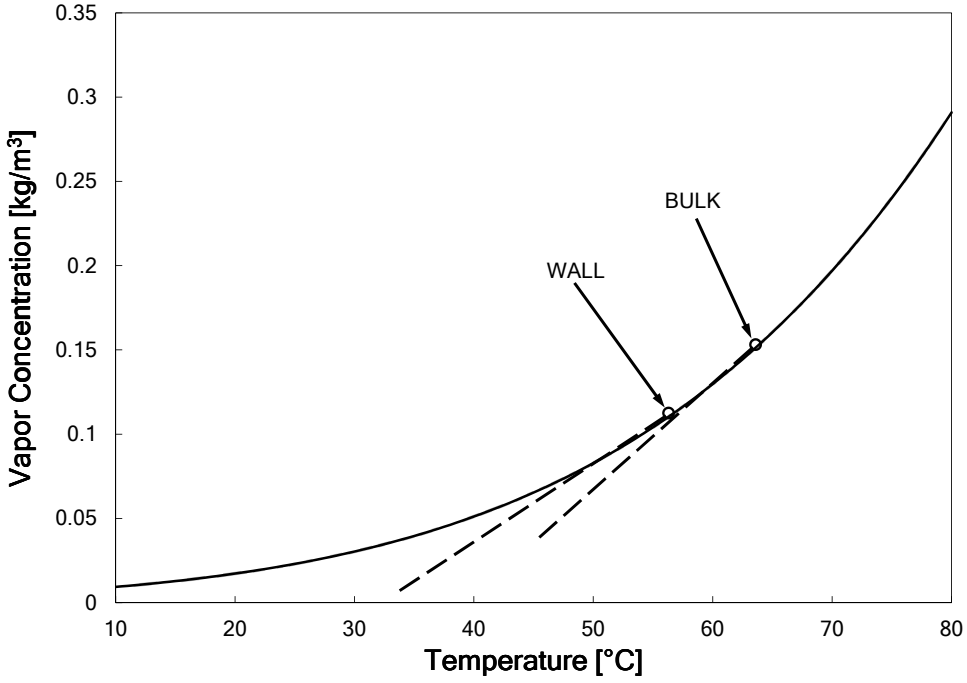

Figure 13: The exponential variation of saturated vapor concentration with temperature means that the bulk and wall states experience locally different curvatures, leading to inherent inequalities in the distribution of entropy generation rate.

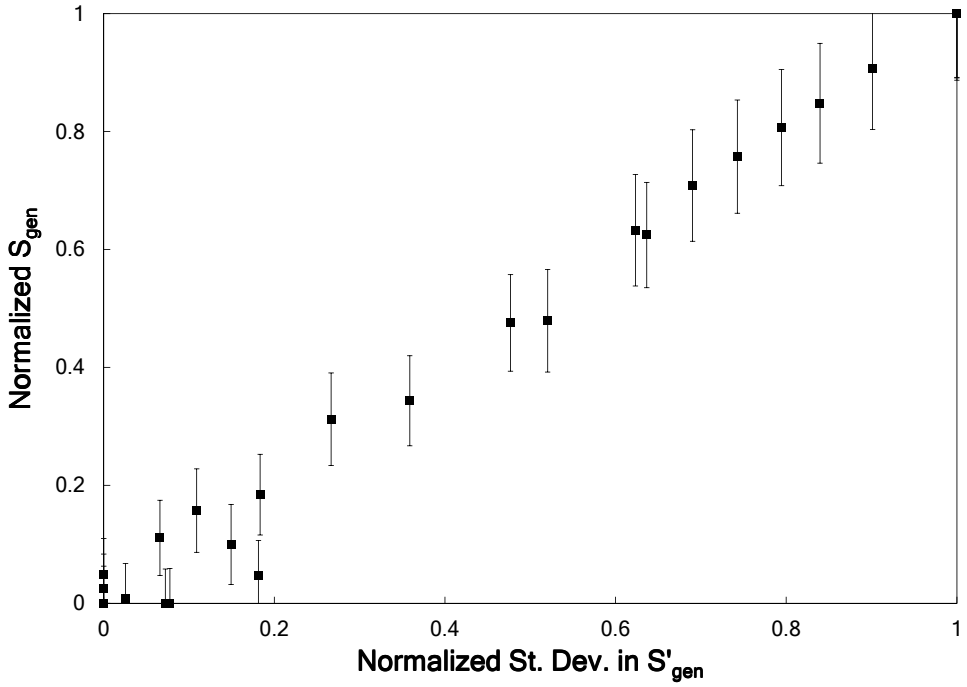

Figure 14: Minimizing the standard deviation (equivalent to variance, as standard deviation is the square root of variance) in local entropy generation rate leads to a global minimum in entropy production rate. Error bars shown are based on the propagation of a maximum 5% uncertainty in dimensional S_{gen} to the normalized values S^{+}_{gen}.

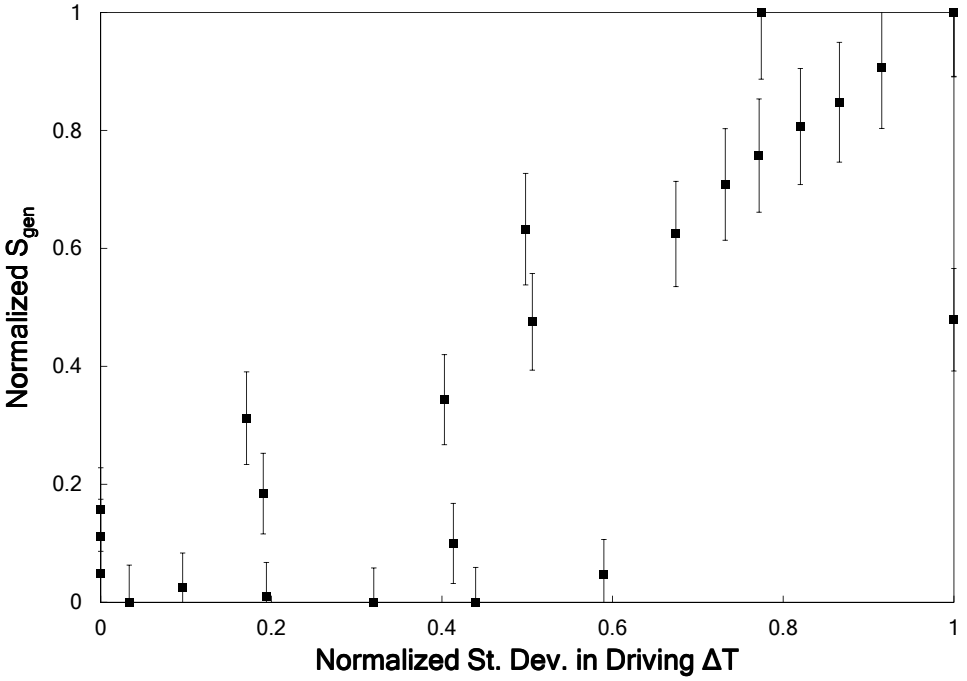

Figure 15: Minimizing the standard deviation in driving temperature difference does not correspond to minimum entropy generation. Error bars shown are based on the propagation of a maximum 5% uncertainty in dimensional S_{gen} to the normalized values S^{+}_{gen}.

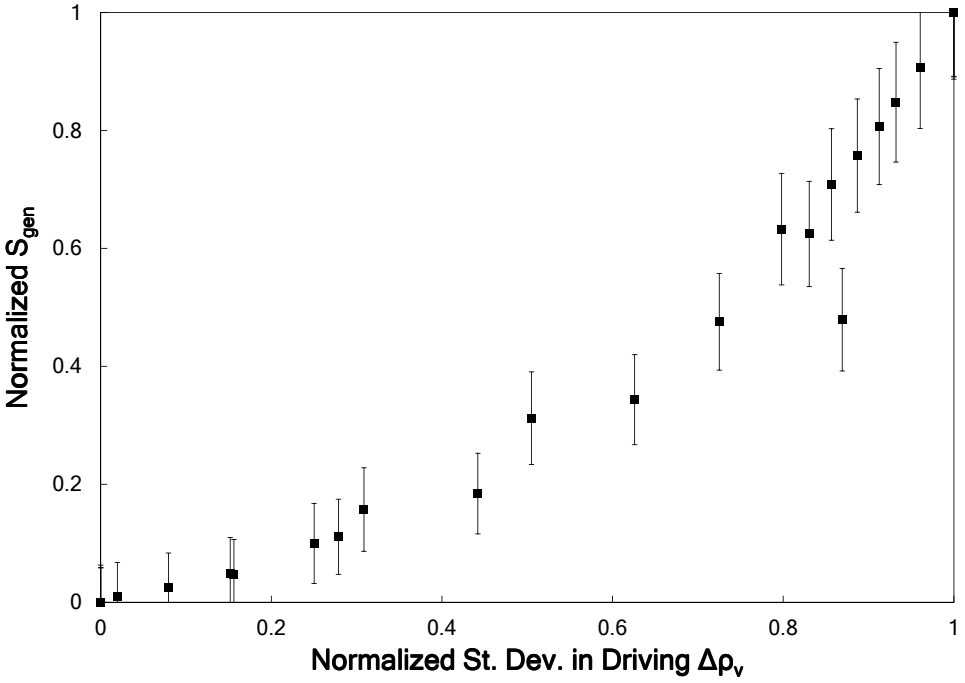

Figure 16: Minimizing the standard deviation in driving partial density difference corresponds well with total minimum entropy generation rate. Error bars shown are based on the propagation of a maximum 5% uncertainty in dimensional S_{gen} to the normalized values S^{+}_{gen}.